SYNTHESIS AND CHARACTERIZATION OF RICE HUSK ASH FOR COLOR ADSORPTION APPLICATIONS

A Thesis Submitted
in Partial Fulfilment of the Requirements
for the Degree of
MASTER OF TECHNOLOGY
by
RAJEEV KUMAR

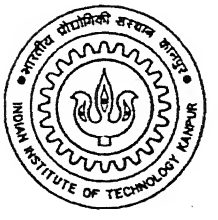

to the
DEPARTMENT OF MATERIALS & METALLURGICAL ENGINEERING
INDIAN INSTITUTE OF TECHNOLOGY KANPUR
APRIL, 1999

CERTIFICATE

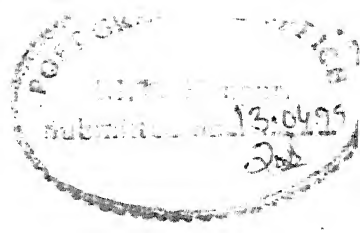

It is certified that the work contained in the thesis entitled **"SYNTHESIS AND CHARACTERIZATION OF RICE HUSK ASH FOR COLOR ADSORPTION APPLICATIONS"** by Rajeev Kumar, has been carried out under my supervision and this work has not been submitted elsewhere for a degree.

13.4.99

Dr.K.N.Rai,
Professor,
Department of Materials Science Programme
and Metallurgical Engineering,
Indian Institute of Technology,
Kanpur. 208016

April, 1999.

Dedicated
to my
Beloved Parents .....

Acknowledgement

I express my gratitude to my thesis supervisor Dr. K. N. Rai for his excellent guidance, constructive advice, constant support and encouragement throughout the present work. It was an unique experience to work under his guidance.

I express my gratitude to all my teachers till now.

I must thank the staff of ACMS workshop for their help during my work. I am also thankful to Sri A.K.Rai for supplying molasses.

I finally thank all my friends specially Karthikeyan, Asutosh, Bhujbal, Somnath, Punya, Anju and Reshu who often shared their time and company with me. They have made my stay at I.I.T. Kanpur a memorable one.

Rajeev Kumar

Abstract

Rice is one of the major crops grown through out the world. After the separation of rice from paddy, one-third mass remains as residue husk. Many workers have tried to use this agricultural waste to produce useful materials such as silica, silicon carbide, activated carbon.

In this present work, an attempt has been made to present all the work done in this area for the last ten years and study the adsorptive power of rice husk ash prepared under different conditions. Three main types of products have been considered viz. (i) husk ash produced in air, (ii) husk ash produced in hydrogen atmosphere and (iii) phosphoric acid activated ash from air fired ash. The characterization of these materials involve X-ray diffraction, scanning microscopy and nitrogen adsorption at liquid nitrogen temperature by BET method. The validation of these products have been evaluated by decolorizing capacity of standard molasses and iodine solution. The adsorptive power of these products have been found to be highest for activated ash and lowest for hydrogenated ash. The total fluctuation from standard activated carbon is within 20% nearly.

Contents

List of Figures

List of Tables

Chapter 1

Introduction

India resides in villages. About 70% of its population lives in rural area and their main occupation is agriculture, contributing to 36% of gross domestic product. Though a large variety of crops are grown, rice is one of the major crops. Out of total area of the world under cultivation for rice, around 29% lies in India, producing 30% of the total rice production. During the separation of rice from paddy, about 30% of the mass is residue husk. This byproduct remains without efficient economic exploitation. Further, uncontrolled littering causes both the storage and environmental problems. This has lead to spurt of investigations through out the world to search for better products based on rice husk. The foregoing sections are therefore devoted to shed light on various aspects of work going on for synthesizing newly and newly products from rice husk. The important investigations in this area are presented below.

1.1 Thermal Degradation of Rice Husk

Thermal Gravimetric Analysis (TGA) of rice husk has been carried out by Teng et al.[1] from room temperature to 1173 K at heating rates of 10, 30, 60 and 100 K/min. From

the TGA, they noticed four different categories of lumps corresponding to the (i) evolution of moisture, (ii) hemicellulose, (iii) cellulose and (iv) lignin. The decomposition of each lump was characterized by a first order reaction with respect to the amount of volatiles present, having an activation energy of 48, 154, 200 and 33 kJ/mol respectively. Differential Thermal Analysis (DTA) of rice husk showed three important endothermic peaks at 370, 420 and 520°C, indicating that silica is present in three locations with different bonding energy[2]. Pyrolysis of rice husk hydrolytic lignin at 100-400°C and a heating rate of 2 deg/min was done by Saprykin et al.[3]. By observing the emission velocities of CH_4, CO and CO_2 with temperature, they determined the temperature range for the formation of carbon oxides and methane. The range for carbon oxides and methane showed a maximum of 320-440°C and 380-450°C respectively. Thermal degradation of rice husk and hydrolytic lignin (from husk) was performed in air and nitrogen. The main components obtained were CO, CO_2 and low molecular weight hydrocarbons[4]. Pulverization of rice husk was done and the changes in husk densities were determined. It was found that morphology of the milled rice husk changed drastically. The densities of milled rice husk was higher and increased with decreasing milled husk sizes[5].

1.2 Rice Husk Silica Production and Properties

Silica is an important ingredient in the production of glasses, cements and other refractories such as porcelain[15]. Normally it is obtained by pulverizing graded quartzite rocks. The powder production is a highly energy intensive process. Unlike this, silica from rice husk can be produced by simply burning under appropriate conditions. The energy is supplied from the carbonaceous part of husk itself. Also, silica produced in this manner is highly reactive, requiring minimum grinding. Therefore, attempt by many workers have been made to produce silica from rice husk. Hayashi et al.[6] have produced silica having large

surface area and high porosity by burning rice husk. During the process about 20% mass of rice husk remains as ash, which contains 95 wt.% silica. High purity silica having purity of 99.99% was produced from rice husk using HNO_3 and H_2O_2 in a definite proportion (rice husk/H_2O_2=1:50 by weight, H_2O_2/HNO_3=10:1 by volume) under optimum conditions (temperature=150°C, time=3 hours)[7]. Cook et al. have produced biogenetic silica by feeding rice husk in an inclined rotatory furnace at 450°C, which was rotated at 1 rpm for 30 minutes[8]. Biogenetic silica of very high permeability was also prepared[9]. It was found by Chakraverty et al. that leaching of rice husk with HCl at 75°C for one hour prior to combustion produces amorphous silica of complete white color[10]. Silica having purity of 92% and average diameter of 0.04 to 0.05 micron was produced by Huang et al.[11]. Their production of silica involved four stages i.e feeding, combustion, spraying and drying. Studies of surface morphology (SEM), chemical reactivity and surface area measurements reveal the formation of amorphous silica during ashing. The reactivity was found to be maximum at ashing temperature range of 400-600°C and holding time of 6-12 hours. However, it was found to decrease with ashing temperature and hold time[12]. After comparing the X-ray photoelectron spectroscopy peak widths of natural silica with those of rice husk ash, the authors[13] have attributed the differences in width due to variation in immediate chemical environment of silica and oxygen in the husk ash.

Rice husk ash produced in this manner can be used as a substitute for natural quartz in the production of porcelain[14]. It can also be used in the production of high silica zeolite of pentasil family[15]. Rice husk formed at 700°C is amorphous and can be used in the production of cristobalite[16]. Because of it's high porosity and large surface area, it can be used to synthesize siliceous raw materials such as clay mineral. Smecite was prepared from rice husk ash using Si, Mg and Li[8]. Biogenetic silica can be used in industrial waste water treatment[9]. Fukazawa[17] has prepared friction materials having balanced energy absorption coefficient and other friction properties by compaction and press sinter-

ing (temperature=750-850°C, pressure=1-10 MPa) of a mixture containing Sn (2-8 wt.%), SiO_2 (2-10 wt.%), graphite (18-33 wt.%), rice husk (2-8 wt.%) and rest electrolytic Cu powder.

1.3 Production of Silicon Carbide Ceramics

Silicon Carbide is an important ceramic used as high temperature material. Rice husk contains both the ingredients (silicon and carbon) necessary for producing silicon carbide. Steam expansion treatment of husk therefore, has been used to produce silicon carbide. The process involved steam expansion (10-30 kg/cm^2) treatment of husk at 150-230°C for 30 minutes followed by hot pressing at 150 kg/cm^2 after pyrolysis at 500-700°C. The above process has been found to be effective in (i) solubilization and depolymerization of rice husk organic substances, (ii) concentration of silica in the treated husk, (iii) decrease in C/SiO_2 ratio of the pyrolyzed residue and (iv) minimization of carbon content in the final silicon carbide ceramic materials[18]. Yoshikawa et al.[19] have produced porous silicon carbide ceramics by coating rice husk powder (40 micron) with a solution of carbonizable thermosetting resin followed by molding, firing (temperature=1500-1800°C, non-oxidizing atmosphere) and refiring in air (to remove residual carbon). High grade silicon carbide of 99.7% purity was prepared by reacting the product obtained after supplying rice husk ash and a binder containing coaltar or high siliceous clay in a gasification furnace at 1700-2100°C with reaction time of 3 hours[20]. Vlasov et al.[21] have attempted to synthesize fine grain powders (1-2 micron) and fibers (apex ratio=5-20) of silicon carbide by treating rice husk and it's hydrolysis product lignin at 500-800°C in nitrogen and air. The reported yield of silicon carbide and lignin was 30% and 40% at optimum SiO_2/C ratio of 1.3. Patel[22] has studied the role of various catalysts (Fe, Co, Ni,Pd) and fluxing agents (Na, K, Cr,Ca) during pyrolysis of husk for silicon carbide whisker production. The effect

of processing variables (calcining temperature, atmosphere and $FeCl_3$ catalyst) on the production of silicon carbide whisker's growth kinetics and phase formation (SiC versus SiO_2) has also been investigated by Martinelli et al.[23]. An attempt[24] to produce ceramic carrier containing 80-92% ceramic materials, 3.5-14.5% combustible substances (wooden fibers, starch, carbon powder and rice husk), 3.5% volatile substances (inorganic carbonates and sulfates) and 1-2% additives has been carried out by calcining these at 1100-1300°C.

Silicon carbide ceramics can be used in variety of applications, such as semiconductor manufacturing furnaces, construction materials and filters[19]. Porous ceramic carrier for immobilization of micro-organisms can be used in petrochemical industries for waste water treatment[24]. Ceramic bricks having very high compressive strength and good water absorption (20%) has been found to be useful in load bearing walls[25].

1.4 Activated and White Carbon Black

Yu et al.[26] have developed a new technique for the production of high quality white carbon black by precipitating hydrated silica ($nSiO_2.xH_2O$) using reaction between carbonized rice husk and Na_2CO_3. The importance of this technique is high yield (90%) of white carbon black and reusablity of Na_2CO_3 solution. Wei et al.[27] have also attempted to produce white carbon black (porous silica) by igniting purified rice husk to whitening combustion in a rotatory furnace. A process for the production of both white and activated carbon was developed by Liu et al.[28]. They produced white carbon by heating a mixture of carbonized rice husk (temperature=600-650°C) and Na_2CO_3 solution (8-11 baume) in ratio of 1:37 for 3-3.5 hours at 120-130°C, followed by neutralization with 25% HCl. This white carbon after acid washing and purifying, was heated at 650°C for 15-18 minutes to produce activated carbon. Granular Activated Carbon (GAC) was produced by Usmani et al.[29] from high and low ash rice husk using $ZnCl_2$. Here $ZnCl_2$ acted both as an

activating agent as well as binder.

The physical (bulk density and hardness) and chemical (pH and mineral content) characteristics of granular activated carbon made from rice straw, pecan shells and hulls of soyabean and rice were found to be useful in raw sugar decolorization[30]. Youseef et al.[31] have studied the surface properties of $ZnCl_2$ on steam activated carbonized (temperature=873 K) rice husks. Specific surface area of the carbon prepared and the changes caused by activation were determined by adsorption of nitrogen at 77 K or carbon dioxide at 298 K and methylene blue from aqueous solution at 303 K.

1.5 Molds and Clays

Molds of rice husk compounded with different substances shows good properties such as compressive strength, heat and warping resistance. Molds of a mixture of cement and dried rice husk (volume ratio= 1 to 3) having water-cement ratio (0.4 to 0.6) were manufactured by Iwayama et al.[32]. They poured the mixture into cylindrical molds and cured it under pressure at a compressive ratio of 1.1 to 1.4. Tough moldings from a mixture of propene polymer (100 parts), maleic anhydride (I)-grafted propene polymer (1-25 parts), glass fibers (5-100 parts) and rice husk (1 -75 parts) were manufactured by Shiraishi et al.[33]. Tough moldings were also manufactured by these workers by pelletizing a mixture of MS 684100, I-grafted polypropene (7 parts) crushed rice husk (10 parts) and glass fibers (30 parts) at $180°C$ followed by injection molding at $220°C$. Molding of a mixture of glutenes (100 parts) with nontoxic polyalcohols hydrophilic plasticizers (15-40 parts) and edible fillers (less than 40 parts) was found to give golf tees[34]. Watanabe et al.[35] have attempted to obtain the compositions for monolithic (magnesium oxide, mullite or chamoite) refractories, by mixing crushed rice husk (1 mm) with (1-100) weight parts of refractory material. 10% aqueous solution of rice husk was used in the manufacture of polymer-bonded clay[36]. Painuli et

al.[37] have studied the use of natural substances (coarse and fine rice husk, sawdust) and synthetic organics (polyvinylalcohols, polyacrylamides and polyvinylacetates) to improve the aggregate stability of sodic sandy loam solids. Rice husk was used as a source of siliceous material for the manufacture of carbon containing silicate molded bodies having density 0.1 g/cm^3, binding strength 6.2 kg/cm^3 and drying shrinkage 0.27%[38].

The above can find important place in many applications. Molds prepared from rice husk and propene polymer was found[33]to show good heat and warping resistance (0.5% warping after 48 hours at 23°C and 50% relative humidity, flexural modulus 38900 kg/cm^2 and heat distortion temperature of 139°C). Dry powdered plant fibers of golf tees can be used as a filler[34]. The use of rice husk in place of conventional fibrous additives improved the flowability, heat insulation and workability of the refractory composites[35]. Polymer bonded clay manufactured from rice husk showed good gloss, water and abrasion resistance. This can be used for surface treatment, waterproofing and mothproofing of articles[36]. The stability of sodic sandy loam solids was found to increase by incorporating rice husk and organics[37]. Concrete surface cleaning compositions were determined by Ookawachi et al.[39] using materials (sawdust, powdered cellulose, powdered rice husk) containing powdered detergents and colorants. Good quality surface decorative and surface finishing boards were prepared by binding rice husk with formaldehyde-urea resin binder or with caustic magnesite powder and $MgCl_2$[40].

1.6 Fertilizer Blends

Various types of fertilizer for agricultural use were prepared from rice husk using different techniques. Coated fertilizer having controlled release has been produced by Yokota et al.[41]. They found that the presence of rice husk slowed down the release of fertilizers. Rice husk was formed into packaging members of pellets, which were found to be biodegradable

and can be used as a fertilizer[42]. Yamada et al.[43] have produced slow release type of fertilizer by heating philippine dolomitic limestone, rice husk and potassium carbonate at 700-900°C in air. For fertilizer to be effective, the molar ratio of $(CaO+MgO+K_2O)/SiO_2$ was found to be in the range of 2.0-2.5.

1.7 Fuel and Process Ingredient (Iron and Cement making)

Rice husk is widely used as a fuel and temperature control agent in various processes. Cast iron feed was produced by the melting of iron base scrap in an electric submerged arc furnace using rice husk. The efficiency was upgraded from 60-65% of a small furnace to 80-90% in a big furnace[44]. Suzuki et al.[45] have used burnt rice husk as a source of carbon to prevent the decrease in temperature of molten pig iron in steel making. Pelletization followed by reduction (CO atmosphere, temperature=1100-1150°C) and purification (sulfur removal) of a mixture of powdered iron ore, rice husk and binder (bentonite) was done. This was found suitable for the production of sponge iron[46]. Barkakati et al.[47] have used the calorific value and reactive silica of rice husk for making portland cement. The use of rice husk decreased the production cost, since it decreased both the fuel and silica consumption. It was observed by sugita et al.[48] that the addition of rice husk to cement not only increased the concrete strength but also it's resistance to 2% HCl solution attack, Cl^-penetration and carbonation. High calorific value of carbonized rice husk decreased the energy consumption of black meal process of cement manufacture by 50%[49]. Use of boiler fired rice husk by Singh et al.[50] resulted in the improvement of clinker quality and reduction of fuel consumption. Rice husk fired at 450°C with portland cement forms pozzolanic cement, which on combination with water and lime at room temperature forms compounds with cementing properties[51]. Composite solid fuels were prepared by mixing

rice husk with combustion aids (dolomite, lime, slag, $NaNO_3$, Fe_2O_3)[52]. Klatt et al.[53] have used rice husk as thermal barrier by packaging it in the hollow areas of building at pressure 200-250 kg/m^3.

1.8 Production of Lignin and Cellulose

Mainly the process of hydrolysis has been carried out to produce lignin, cellulose and other related products. Kaglunova et al.[54] have carried out demethoxylated lignin catalyzed hydrogenolysis of protolignin, hydrolytic lignin and dioxane lignin from rice husk. They found that the demethoxylated lignin catalyst acted similarly to other catalysts used for above purpose. Moya et al.[55] have attained the maximum benzylation functionalization and yield of lignocellulosic wastes (pineapple peel, rice husks, sawdust) by treatment of $NaOH$ slurries at 90-100°C for 8 hours. This was further dried, milled to a particle size of 0.25 mm. The cellulosic material obtained after extraction was bleached with 2.5% $NaClO$ solution for 4 hours at ambient temperature. The degree of benzylation was determined by infra-red spectra of the cellulosic material. Conditions for cellulose production and other hydrolysis product from rice husk has been investigated by Wang et al.[56]. The optimum conditions for cellulose production were reported as follows:

(a) ratio of straw to wheat barn=7:3,

(b) water content of the solid state medium of straw powder and wheat barn=250 %,

(c) pH =6.0 to 6.5,

(d) temperature=30°C and

(e) incubation time=3 days.

The optimum conditions for the hydrolysis of rice husk were found to be :

(a) proportion of barn to rice husk=1:3,

(b) temperature 40°C,

(c) pH =4.4 and

(d) incubation time=3 days.

Extraction of rice husk with hot water was found to give a polysaccharide, which on hydrolysis resulted in the formation of D-mannose, D-glucose, L-rhamnose and D-galactose. On carrying out methylation followed by hydrolysis, preparation of alditol acetates and gas-liquid chromatography, it was found that the D-mannose, D-glucose, L-rhamnose and D-galactose units are 1,4 linked with D-mannose unit at the terminal[57]. Hydrolysis of rice husk with oligosaccharides containing extraction water was carried out by Filatova et al.[58]. Due to the conversion of oligosaccharides to monosaccharides, hydrolyzate was found to contain higher amount of monosaccharides. The kinetics of acid catalyzed hydrolysis of hemicellulose-polysaccharide complexes obtained from husk of sunflower, rice and cotton has been studied by Statalov et al.[59].

Hydrolysis product obtained from rice husk can be used for many applications. Benzylated lignocellulosic materials can be used in the manufacture of plastics[55]. Rice husk hydrolyzate obtained in presence of oligosaccharides extraction water can be a good raw material for the manufacture of fodder yeast[58]. Cellulosic materials obtained from rice husk can be used to remove Ni and Cu ions from solution[60].

1.9 Production of Organic Compounds

Many organic compounds were synthesized using rice husk. A model for the manufacture of furfural by direct hydrolysis of wood particles or rice or sunflower husks in steam was developed by Sobolev et al.[61]. Oxalic acid in high yield and purity was manufactured by Mane et al.[62] by oxidizing agricultural wastes with conc. HNO_3 in presence of conc. H_2SO_4 and V_2O_5. Pyrolytic oils containing napthalene, fluorene and phenanthrene were obtained during the pyrolysis of wood wastes, municipal solid waste and rice husk in a

glass-purged static batch reactor and a fluidized bed reactor. The oils were separated into different classes[63]. Various amounts of phenols, neutral compounds and acids were also obtained during the pyrolysis of rice husk at 300-800°C[64].

1.10 Production of Inorganic Compounds

Rice husk can be used as a raw material for the production of many inorganic compounds. Suda et al.[65] have manufactured silicic acid by immersing chaff in heated solution of 2% $NaClO$ and 4% $NaOH$ followed by the addition of conc. H_2SO_4. Calcium hydrogen phosphate was produced as a byproduct (yield=10%) during separation of vegetable casein from chaff[66]. Both the alpha and beta phases devoid of fibers of Si_3N_4 was prepared from acid treated rice husk by patel et al.[67]. The lack of fibers was due to the absence of fiber substrates in rice husk which were degraded during acid digestion. Si_3N_4 fibers were obtained by continuously moving rice husk inside a heating zone at temperature of 1300°C in nitrogen atmosphere[68]. Chen et al.[69] have used rice husk's carbon and silica for the production of $SiCl_4$. High purity silicon was produced from the ash of rice husk by acid leaching, ashing at 620°C and thermal reduction in presence of Mg[70, 71]. Nandi et al.[72] have used magnesium silicide from rice husk for the production of silanes. They also optimized acid concentration, temperature and particle size of magnesium silicide for the production of silanes. Rice husk ash was used as a source of silica for the production of choline chloride powder[73]and high crystallinity zeolites ($ZSM-5$ and $ZSM-48$)[74]. Popoola et al.[75] have manufactured a series of dyes based on sulphur chromophores using baking process involving rice husk. Wallastonite was manufactured from rice husk ash by Hevia et al.[76]. Here rice husk was used because of two reasons; firstly it provides silica and secondly it is more economical and easily available.

1.11 Gasification for Power Generation

Salvi[77] has attempted to study the rice husk gasification for power generation. He installed a down flow fluidized bed gasifier, equipped with a rotating grid at the bottom for continuous removal of ashes. The gasification was carried out at temperature of $1000°C$. The process consumed 150-160 kg. of rice husk per hour, giving rise to fuel gas yield of 350 m^3/hr with a heating value of 1000 kcal/m^3. The gas obtained was purified by filtering through rice husk and was fed into an otto generator with controlled combustion to generate 80 KWe. Chowdhary et al.[78] have developed a mathematical model to study the kinetics and mechanism of reactions occurring during gasification of rice husk. The simulated temperature profile and gas composition were compared with a cylindrical updraft moving bed gasifier. Following were the gasification conditions : gasification rate of 3.5-12.5 at 10-30 kg/m^2s and air flow rate of 0.07-0.11 m/s for generation of producer gas with heating value of 3712-4464 kJ/m^3. Model was found suitable for the representation of engineering processes. Nijaguna et al.[79] have built an atmospheric pressure fluidized bed combustor for the utilization of charcoal and agricultural wastes (coconut shell, bagasse, sawdust and rice husk) with air as fluidizing agent and sand as support for fuels. A model of an open core down draft moving bed rice husk gasifier was developed by Manurung et al.[80] to predict its performance as a function of operating variables like heating rate, feed properties etc. The model was based on mass and energy balances, reaction kinetics, transport rates and fundamental thermodynamic relations. The electric power generated can be used as a stand alone system especially for rural areas[77]. The open core down draft moving bed rice husk gasifier model can be used to predict the effect of changing operating parameters and feed properties[76].

Chapter 2

Principles of Experiments

Internal surface area, pore size distribution and porosity are very important properties of powder and porous materials because these properties affect various physical and chemical processes. These properties can not be visually measured by optical or electron optical metallography as such. This section is therefore devoted to present gas adsorption methods involved in the measurements of above properties and also to give a brief explanation of the principles of other various experiments used in this work. Here we only approach a thumbnail sketch appropriate for this work and as much necessary for the discussion of results[81, 82, 83].

2.1 Surface Area Measurements

The most common method of measuring surface area is that developed by Brunauer, Emmett and Teller *(BET)*. They derived following equation for adsorption isotherm relating the volume V of adsorbed molecules in equilibrium with the pressure P of the molecules in the gas phase.

$$\frac{P}{V(P_o-P)} = \frac{1}{CV_m} + \frac{C-1}{CV_m}\frac{P}{P_o}$$

where,

P_o = saturation pressure of adsorbate gas at the experimental temperature,

V = volume of gas adsorbed at pressure P,

V_m = volume of gas adsorbed in monolayer,

C = a constant.

A plot of $\frac{P}{V(P_o-P)}$ versus $\frac{P}{P_o}$ gives a straight line with slope $s = \frac{C-1}{CV_m}$and intercept $i = \frac{1}{CV_m}$. The inverse of the sum of these two gives the volume of gas adsorbed in monolayer i.e V_m on the surface. On substituting the value of V_m in intercept, one can obtain the value of C. From V_m one can calculate the number of molecules adsorbed n,

$$n = \frac{V_m N_o}{22414}$$

From this, surface area per gram S can be calculated by multiplying n with area occupied by one molecule of adsorbent, divided by the mass of material m under investigation.

$$S = \frac{V_m N_o A_m}{22414m} \times 10^{-20}\mathrm{m}^2$$

N_o=Avogadro number,

A_m=Area occupied by one molecule of adsorbent.

For Nitrogen at it s boiling point, the value of A_m used is 16.2 A^{o2}.

2.2 Pore Size Distribution

Measurements of the amount of gas adsorbed or desorbed as a function of reduced pressure $\frac{P}{P_o}$ provides the most common procedure for the determination of pore size distribution of fine pores. The basic principle is that the pressure at which vapor will condense into liquid of surface tension σ is determined by the curvature of the meniscus r_k of the condensed liquid in the pores. This is given by the following Kelvin equation for the variation of vapor pressure with surface curvature in a capillary tube closed at one end,

$$ln\frac{P}{P_o} = \frac{-2\sigma V_m \cos\theta}{r_k RT}$$

where,

P_o= vapor pressure of liquid over a plane surface,

σ= surface tension of the liquid adsorbate,

θ= contact angle,

r_k= radius of curvature,

r_c= physical radius of cylindrical pore,

R= gas constant,

T= absolute temperature.

Consider a porous solid in contact with a vapor at some relative pressure $\frac{P}{P_o}$. A vapor which wets the surface ($\theta = 90°$), such as nitrogen is chosen so that $\cos\theta = 1$. An adsorbed layer of thickness t will already be present on the walls of all unfilled capillaries. It is therefore assumed that the radius of meniscus in the unfilled pores is not the true physical radius r_c but rather than this has been diminished by the thickness of the adsorbed layer and therefore $r_k = r_c - t$. The critical radius r_c will be related to reduced pressure by the expression,

$$r_c = \frac{-2\sigma V_m}{RTln(P/P_o)} + t$$

The main problem in obtaining r_c lies in knowing the value of t. The most direct method of determining t is to measure the adsorption isotherm of the same gas on a non-porous reference substance having surface as nearly identical in nature with the porous substance. Next, it is assumed that at the same relative pressure the thickness of the multilayer on this non-porous solid is the same as the thickness of the film in the pore. If t_m is the thickness of a single layer, then the total thickness $t = nt_m$,where n is the number of layers. For calculating the value of t , it is assumed that the molecules are rigid spheres and the stacking is hexagonal closed packed. The mass of nitrogen adsorbed per cm^2 is,

$$\frac{28}{16.2\times10^{-16}\times6.023\times10^{23}}$$

where 16.2 $A^{\circ\,2}$ is the area of one nitrogen molecule. It s liquid volume can be calculated

by assuming it to have the normal density of bulk liquid nitrogen which corresponds to hexagonal packing. The volume is,

$$\frac{28}{16.2\times10^{-16}\times6.023\times10^{23}}\times\frac{1}{0.81}= 3.5 \times 10^{-8}\text{cm}^3$$

Since the area considered is one cm^2, the thickness $t_m = 3.5$ A°. So, from t_m, t can be obtained at various values of $\frac{P}{P_o}$. Nitrogen adsorption has been used almost universally, and the values of t as a function of $\frac{P}{P_o}$ has been estimated by a number of investigators who have worked with non-porous substances of known area. Values of t are essentially independent of the chemical nature of the adsorbent for most systems at coverage greater than a monolayer. Table-(2.1) gives the relationship published by three group of investigators.

2.3 Determination of Energy of Activation

Energy of activation can be determined from surface area measurements using following expression,

$$\ln \frac{\dot{A_2}}{\dot{A_1}} = -\frac{\triangle E_a}{R}[\frac{1}{T_2} - \frac{1}{T_1}]$$

where,

$\triangle E_a$ =heat of reaction,

$\dot{A_2}$ = change in surface area per second at temperature T_2,

$\dot{A_1}$ =change in surface area per second at temperature T_1.

A plot of $\ln A$ with $1/T$ will give a straight line having slope= $-\frac{\triangle E_a}{R}$. By knowing the slope, $\triangle E_a$ can be calculated using the following expression,

$$\triangle E_a = -R \times slope$$

Table 2.1: Values of t at different $\frac{P}{P_o}$ as determined by three group of investigators

P/P_o	Cranston and Inkley	deBoer etal	Gregg and Sing
0	0	-	-
0.05	0.339	-	-
0.10	0.412	0.368	-
0.20	0.485	0.436	-
0.30	0.567	0.501	0.56
0.40	0.635	-	0.62
0.50	0.70	-	0.68
0.60	0.75	0.736	0.75
0.70	0.86	-	0.85
0.80	1.00	-	0.98
0.90	1.22	-	1.27
0.95	1.40	-	1.63

2.4 Pore Volume Determination

Total pore volume is determined by measuring the total adsorbate volume at a relative pressure as close to unity to include the large radii pores in the measurement. If W_a gm of nitrogen is adsorbed at $\frac{P}{P_o} = 0.99$, then the corresponding volume of pores V_p is given by,

$$V_p = \frac{W_a}{\rho_l}$$

where ρ_l is the density of liquid nitrogen.

2.5 Liquid Impregnation Technique

In some cases, it is not possible to determine the total pore volume by nitrogen adsorption method because samples keep adsorbing nitrogen for a long time. Thus, adsorption remains incomplete. In those cases, liquid impregnation technique is used. In this method, small amount of sample is taken on a glass slide and is weighed. The sample is then impregnated by a volatile liquid of known density, such as acetone (ρ =0.8 gm/cm^3). This is left for some time till the liquid just volatilizes from the surface of the slide and sample. The liquid in the pores however do not volatilizes and remains impregnated in the pores. The

weight of the liquid is determined in the impregnated state after subtracting the weight of the slide and dry sample, as determined earlier. By dividing the weight of the liquid with it s density, the volume of liquid which is equal to pore volume of sample is calculated.

2.6 X-Ray Diffraction

X-Ray diffraction can be used to obtain information about the location and arrangement of atoms in the solid constituting the crystalline materials. Common compounds can be identified using ASTM powder diffraction pattern. With calibration procedures, it is possible to obtain quantitative information and thus approximate amount of a particular phase in a sample can be determined. The mean crystalline size of a material can also be determined from the broadening of X-ray diffraction peak. The line broadening is inversely proportional to crystallite size and can be used to give average microcrystalline size down to 3 to 10 nm with an upper limit of 1 micron.

2.7 Scanning Electron Microscopy (SEM)

Scanning microscopy has been used primarily to examine the topology of surfaces. In Scanning Electron Microscope (SEM), the electron optics act before the specimen is reached to convert the beam into a fine probe which can be as small as 100 $A°$ in diameter at the specimen surface. As the probe is scanned over the specimen surface by deflection coils, an image may be formed by collecting in a detector any suitable signal (backscattered electrons, emitted X-rays or optical photons) and displaying this signal in a raster synchronous with that of probe. The incident electron beam causes the emission of secondary electrons, auger electrons and characteristic X-rays that can be analyzed to provide additional information about the same area of the sample on which a SEM picture is obtained.

Chapter 3

Experimental Procedure

This section gives a brief description about various experimental procedures adopted in the production and characterization of different categories of rice husk ash.

3.1 Sample Preparation

Three different categories of ash has been prepared in the present investigation from rice husk under following conditions.

(a) Ambient atmosphere production,

(b) Production under hydrogen atmosphere and

(c) Ash activation by phosphoric acid.

3.1.1 Ambient Atmospheric Production

Four samples were prepared by charring rice husk (kept in silica crucible) at four different temperatures i.e 400, 600, 750 and 900°C followed by atmospheric cooling, after withdrawing the samples from furnace temperatures.

3.1.2 Production Under Hydrogen Atmosphere

In the present case, the rice husk samples were kept in a silica crucible hanging in silica tube placed outside the furnace. When furnace reached desired temperature, the silica tube containing sample was lowered in the desired heating zone of the furnace after flushing it with hydrogen. The flow of hydrogen was continued till desired time of one hour.The silica tube after holding time of one hour was withdrawn slowly from the furnace and cooled finally in atmosphere to room temperature.

3.1.3 Ash Activation by Phosphoric Acid

TGA of rice husk [Fig.-(3.1)] was taken in air at heating rate of 10 deg /min. This shows that the maximum mass loss takes place between 300 to 400°C. Surface area of all the samples prepared above were determined. The surface area was found to be maximum for the sample prepared in air at 400°C. Keeping in mind the above results, an attempt to produce activated husk from rice husk was proceeded in the following way.

First of all rice husk was charred in air by keeping the crucible containing rice husk in the furnace at 300°C for one hour followed by atmospheric cooling to room temperature. 20% of orthophosphoric acid (BDH lab. reagents) was added to the charred product in a 250 ml. beaker with stirring. After which it was left for one day to allow sufficient time for the absorption of orthophosphoric acid by the charred product. Resultant mixture was dried completely by heating (temperature=65-70°C) followed by keeping in furnace at 300°C for one hour. Small amount of the newly formed char was taken in a long silica tube and was heated in vacuum for four hours at five different temperatures 600, 700, 800, 900 and 1000°C. Thus five samples of activated husk were prepared.

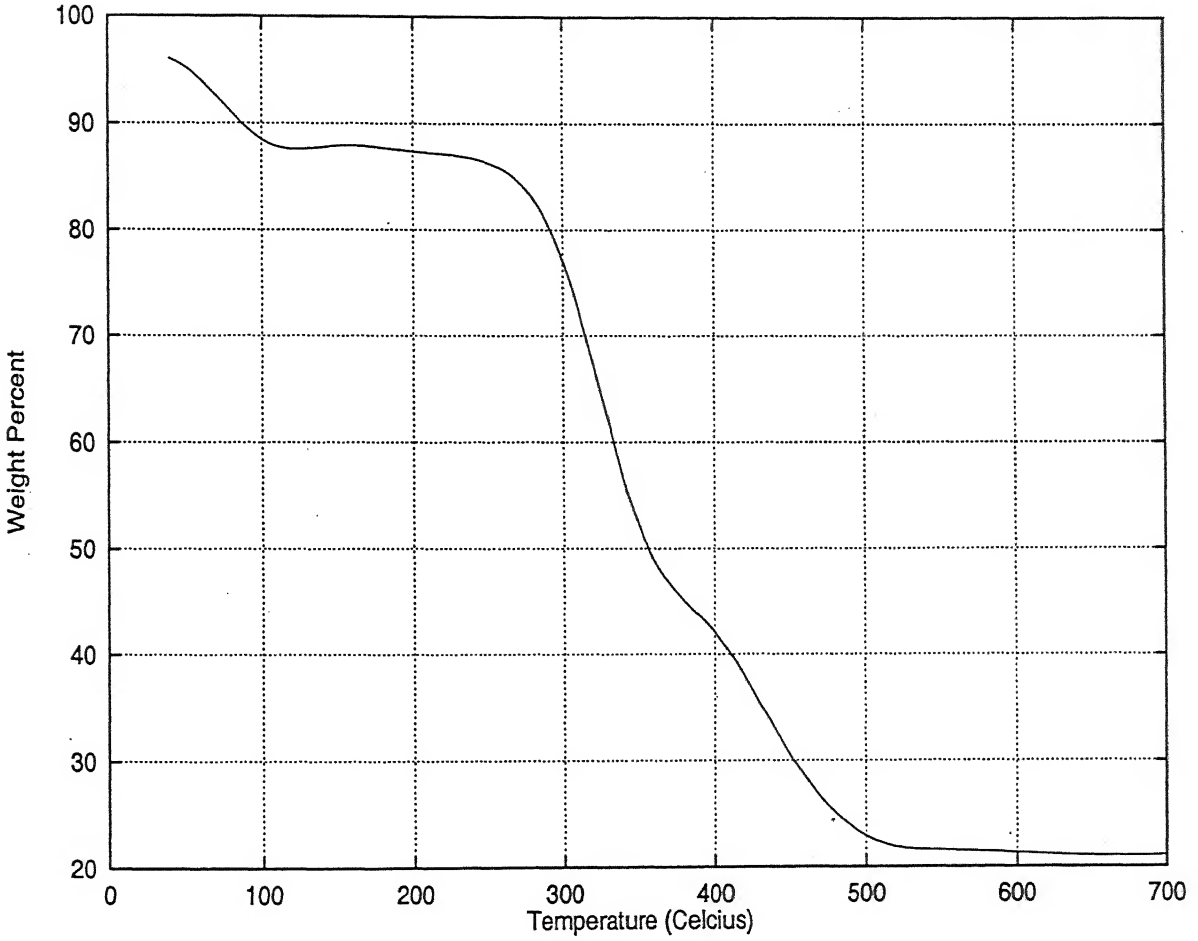

Figure 3.1: TGA of rice husk in air at heating rate of 10 deg/min.

3.2 BET Parameters Determination

BET parameters such as surface area and pore volume of all the samples were determined by BET method by nitrogen adsorption at liquid nitrogen temperature, as described in section (2.1 to 2.4). For this COULTERtm SA3100tm Series Surface Area and Pore size Analyzer was used.

3.3 X-Ray Diffraction

X-ray diffraction pattern of all the samples were recorded by ISO-DEBYEFLEX 2002 from 2θ range of 10 to 120. Diffraction patterns were recorded under following conditions.

Table 3.1: Parameters used for recording X-ray diffraction patterns

X-ray Source	Cu K_α
Scanning Speed	3 deg/min in 2θ
Chart Speed	30 mm/min
Counts per min.	5 K
Time Constant	10 sec.
Current/Volt	20 mA / 30 KV

3.4 Scanning Electron Microscopy (SEM) Analysis

JEOL JSM-840A Scanning Microscope was used to take photographs of the samples at different magnifications (120, 500 and 600). The powdered samples were mounted on the step by acetone or graphite paint followed by coating with $Au - Pd$ plasma to make it conducting. Samples prepared in air and hydrogen were also analyzed for silicon, potassium, calcium and iron.

3.5 Chemical Activity Measurements

Chemical activity was determined by the adsorption capacity of all the three types of the samples having maximum surface area. This was accomplished by the decolorization capacity of the samples on standard aqueous solutions of molasses and iodine due to adsorption.

3.5.1 Molasses Test

The aqueous solution of molasses were prepared by dissolving 100 gm of molasses (Kishan Cooperative Sugar Mills, Tahsil-Ghosi, Distt.-Mau, U.P) with 15 gm of disodium hydrogen phosphate (Merck lab. reagents) in 500 ml of distilled water followed by the addition of 20 % orthophophoric acid in order to adjust the pH of mixture to 6.5. The above solution was further diluted to 1 liter. Thus produced standard solution (actually one-tenth of original molasses strength) was assumed to contain 100 units of parent color per 100 ml liquor. A series of solutions were prepared by further diluting 5, 10, 15 to 60 ml of the above solution to 100 ml with distilled water. The color of these diluted solutions therefore correspond to 5, 10, 15 to 60 % of the original solution. Thus, if 10 ml of standard solution is diluted to 100 ml with distilled water, the color of that mixture would represent a concentration of 10 color units per 100 ml. These solutions were used as reference solutions for comparison of colors.

The molasses test was performed on the samples produced (having maximum surface area) by three different methods.

(a) Ash produced in air at $400°C$.

(b) Ash produced in hydrogen atmosphere at $900°C$.

(c) Activated husk produced at $800°C$.

For performing molasses test, 0.5 gm of the sample was added to 50 ml of standard solution followed by stirring and heating to boil. This was kept for 30 minutes to allow

sufficient time for adsorption. The resulting mixture was filtered through whatman no. 5 filter paper. The color of the filtrate thus obtained was matched with the reference solutions prepared earlier. The difference in the color units between standard and reference solution gave the percentage of color adsorbed by 0.5 gm of sample. The same procedure was repeated with 0.3, and 0.1 gm of sample and the percentage of color adsorbed was noted.

3.5.2 Iodine Test

Iodine test was performed exactly the same way as molasses test. However, the preparation of standard iodine solution was done by dissolving 4.1 gm of potassium iodide (Thomas Baker & Co.) and 2.7 gm of iodine (S.D.Fine Chemicals) in one liter of water.

3.5.3 Effect of Time

To carry on time dependent color adsorption study of molasses solution by activated husk ash, 0.5 gm of activated husk ash was added to 50 ml of standard molasses solution in a 100 ml beaker followed by stirring with a glass rod. This was left for 10 minutes and then filtered through whatman no.5 filter paper. The color of filtrate thus obtained was matched with reference solution (preparation of which is given in section 3.5.1) and the percent decolorization of molasses solution was noted. The same procedure was repeated with adsorption time of 20, 30 and 40 minutes respectively. Above experiment was again repeated with 0.3 gm of activated husk ash.

Chapter 4

Results and Discussions

Rice husk ash has been prepared by charring husk in air and in hydrogen atmosphere.The ash prepared in the present exploration was investigated by using techniques of Scanning Electron Microscopy (SEM), X-Ray Diffraction (XRD), BET and Chemical Activity . The results of these studies and associated discussions are presented in the following sections under corresponding headings.

4.1 Rice Husk Ash Produced by Atmospheric Burning

Rice husk char produced in air was characterized for structure, surface area and chemical activity. The results of these studies are presented below.

4.1.1 X-Ray Diffraction

X-ray diffraction pattern of all the samples [(Fig.-(4.1)] do not show well defined peaks. In all cases, a hump is observed in the 2θ range of 16 to 39, indicating disordered structure.

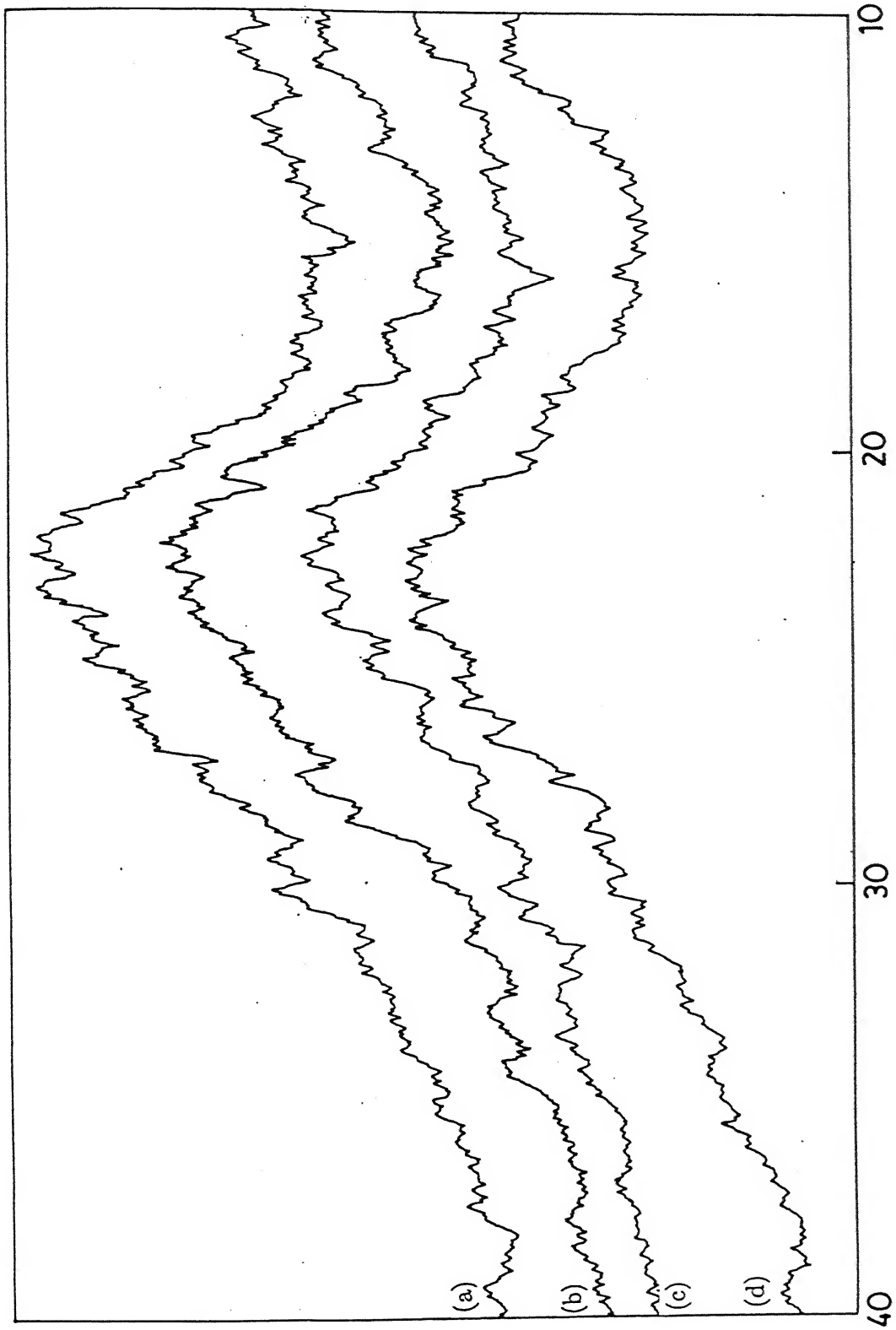

Figure 4.1: X-ray diffraction of rice husk ash produced in air at (a) 400°C, (b) 600°C, (c) 750°C and (d) 900°C

4.1.2 BET (Surface Area and Pore Volume)

Surface area and pore volume observation of various samples are presented in the Table-(4.1) below.

Table 4.1: Surface area and pore volume of rice husk ash produced in air

Husk Burning Temp. ($^{\circ}C$)	Surface Area (m^2/gm)	Pore Volume (ml/gm)
400	178.84	0.1630
600	111.68	0.2398
750	94.12	0.2588*
900	14.22	0.3453*

[* Determined by liquid (acetone, $\rho = 0.8$ gm/cm^3) impregnation technique.]

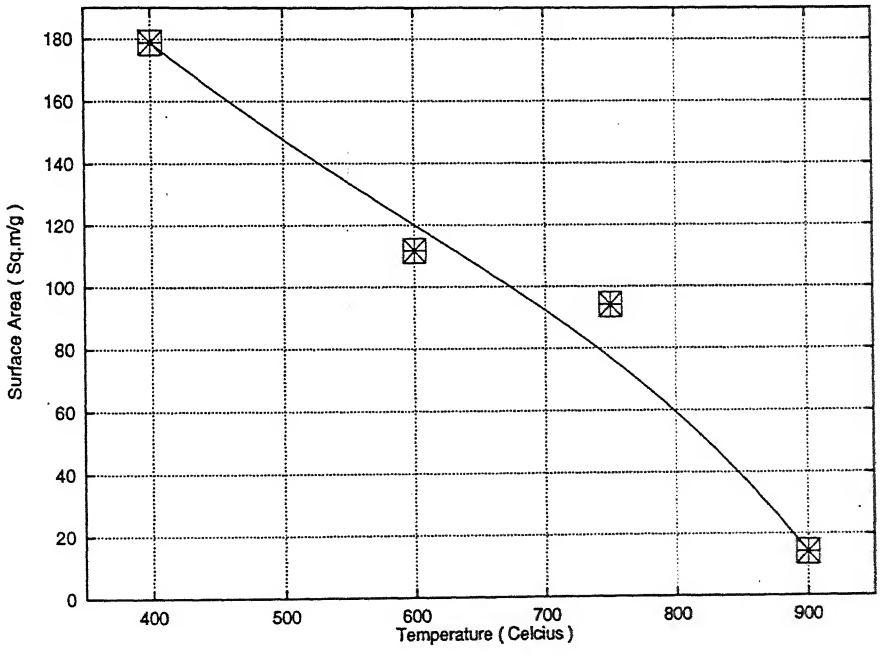

Figure 4.2: Variation of surface area with temperature of rice husk ash produced in air.

The plot between surface area and temperature is shown in Fig-(4.2). It is evident that specific surface area decreases with temperature. The behavior of porosity with temperature shown in Fig-(4.3), shows an increasing trend with temperature.

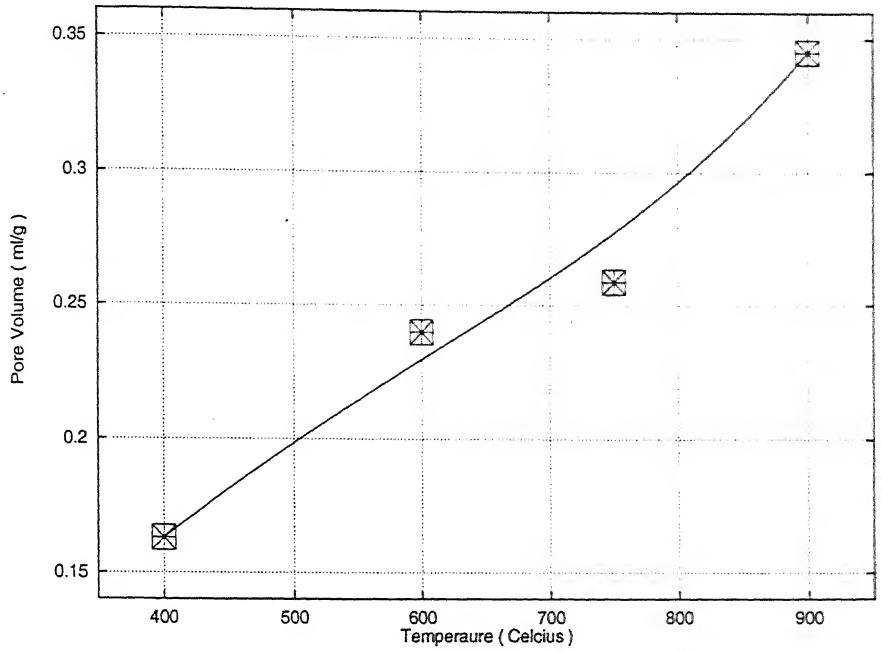

Figure 4.3: Variation of pore volume with temperature of rice husk ash produced in air.

This result along with surface area decrease with temperature could be explained, if we assume the enhancement of void space by pore collapse due to diffusion with rising temperature. This observation is also supported by changes in microstructure (showing larger cavities) of rice husk ash with increasing temperature as shown in Fig-(4.7).

4.1.3 Energy of Activation

Table 4.2: lnA values of rice husk ash produced in air

T (°C)	T (K)	1/T×10^3 K^{-1}	A	$\dot{A}$=A/3600	ln$\dot{A}$
400	673	1.485	178.84	0.0490	-3.002
600	873	1.145	111.68	0.0310	-3.473
750	1023	0.977	94.12	0.0261	-3.644
900	1173	0.852	14.21	0.0039	-5.535

The variation of ln$\dot{A}$ with 1/T is shown in Fig-(4.4). From the figure, value of slope at lower and higher temperature is found to be 1.38×10^3 and 15.13×10^3 respectively. The

corresponding values of $\triangle E_a$ are -11.47 kJ/mol and -125.77 kJ/mol respectively. The value of $\triangle E_a$ becomes more negative at higher temperature, which suggests that the process becomes increasingly exothermic with increasing temperature. This may be due to either change in mechanism during charring or some other chemical reactions which starts taking place at higher temperature.

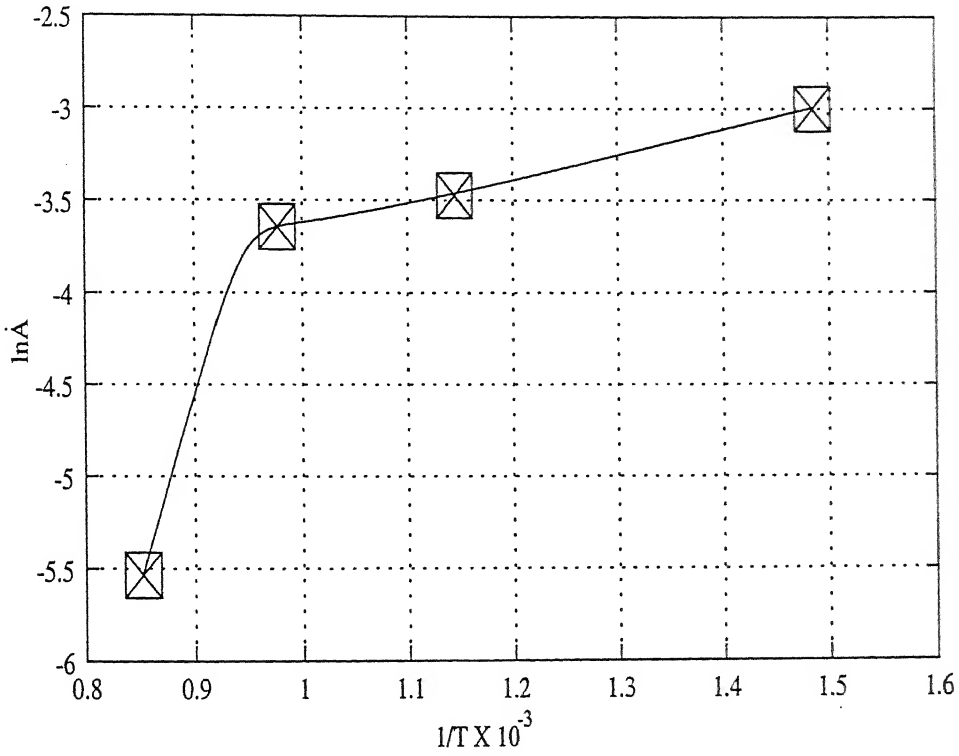

Figure 4.4: Variation of lnA with 1/T of rice husk ash produced in air.

4.1.4 Elemental Analysis

The elemental analysis of rice husk ash samples prepared at various temperatures is shown in Table-(4.3) below. Mainly elements silicon, potassium, calcium and iron were considered. The variation of weight percent of these elements in samples produced at different temperatures is shown in Fig-(4.5) and Fig-(4.6).

Table 4.3: Weight percent of silicon, potassium, calcium and iron in rice husk ash produced in air

Husk Burning Temp (°C)	Si (wt.%)	K (wt.%)	Ca (wt.%)	Fe (wt.%)
400	59.87	15.64	6.24	18.25
600	85.54	7.60	0.87	5.99
750	89.48	4.59	1.82	4.10
900	81.98	9.61	1.62	6.79

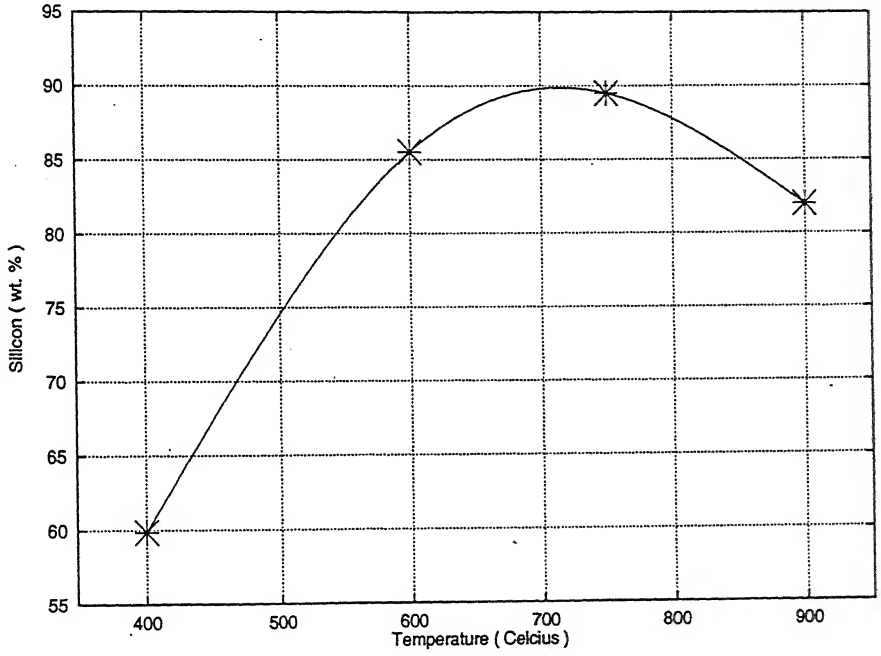

Figure 4.5: Variation of weight percent of silicon with temperature in rice husk ash produced in air.

Fig-(4.5) shows continuously increasing concentration of silicon, in contrast to decreasing trend of remaining three elements [Fig-(4.6)]. It seems that potassium, calcium and iron are present in some form of hydrated salts which sublimates with increasing process temperature. Specially potassium oxide is known to sublimate slowly with increasing temperature. It may be that potassium, calcium and iron all are in some complex form, which on increasing process temperature comes out of the silica matrix leading to apparent enhancement of silicon.

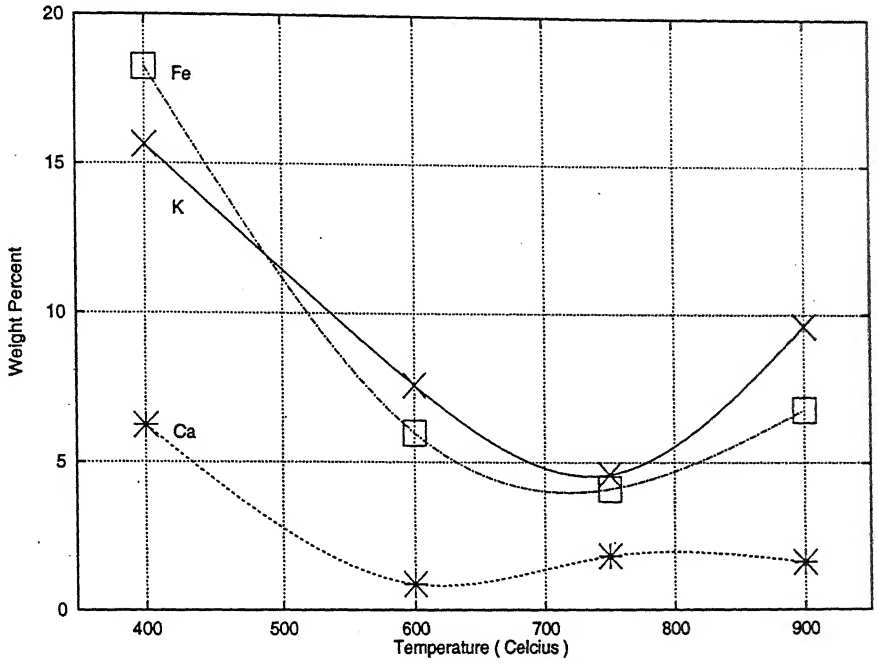

Figure 4.6: Variation of weight percent of potassium, calcium and iron with temperature in rice husk ash produced in air

4.1.5 SEM Microstructure

Scanning electron micrographs for samples prepared at various temperatures are shown in Fig-(4.7). The microstructure corresponding to sample prepared at $400°C$ exhibits network pattern containing porous structure. However, microstructures corresponding to samples prepared at higher temperatures gradually shows collapsed and more planar rigid humpy circular cavity like structure resulting into relatively plane areas. This leads to reduction in number of pores on expense of the formation of circular cavity with large voids. This observation is in contrast to surface area decrease in carbonaceous matrix due to anhilation of pores as a result of cavity formation due to oxidation.

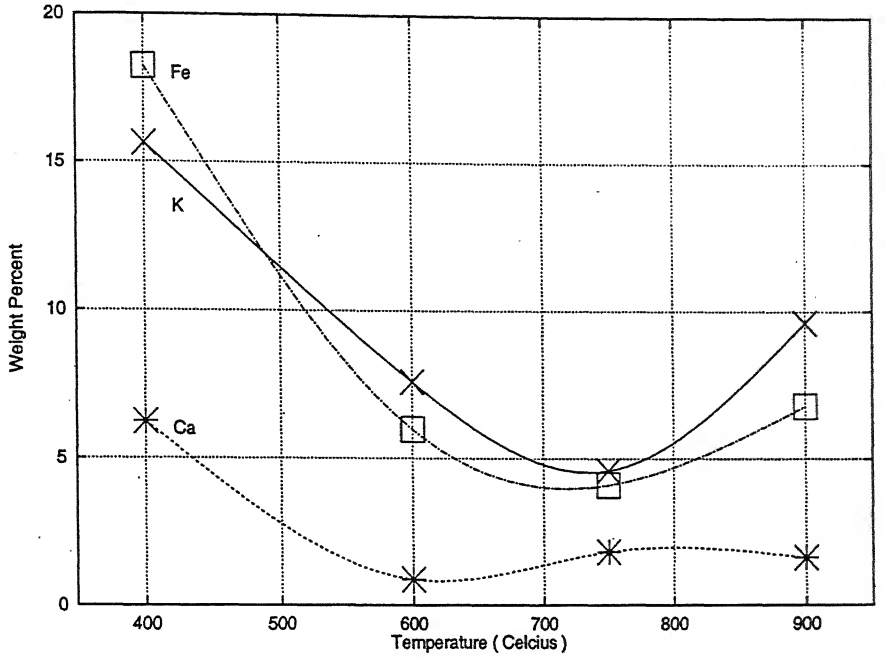

Figure 4.6: Variation of weight percent of potassium, calcium and iron with temperature in rice husk ash produced in air

4.1.5 SEM Microstructure

Scanning electron micrographs for samples prepared at various temperatures are shown in Fig-(4.7). The microstructure corresponding to sample prepared at $400°C$ exhibits network pattern containing porous structure. However, microstructures corresponding to samples prepared at higher temperatures gradually shows collapsed and more planar rigid humpy circular cavity like structure resulting into relatively plane areas. This leads to reduction in number of pores on expense of the formation of circular cavity with large voids. This observation is in contrast to surface area decrease in carbonaceous matrix due to anhilation of pores as a result of cavity formation due to oxidation.

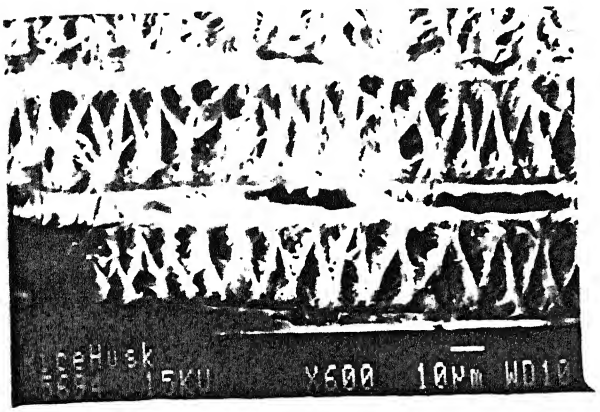

(a)

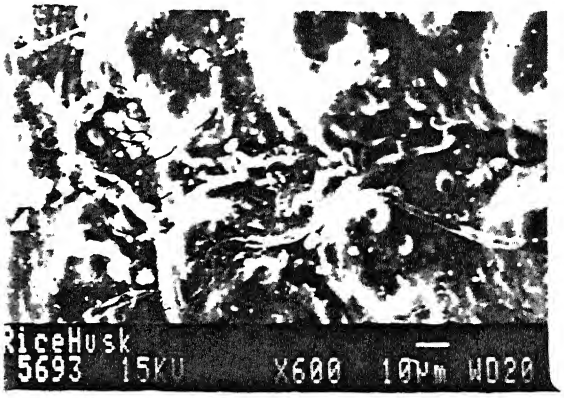

(b)

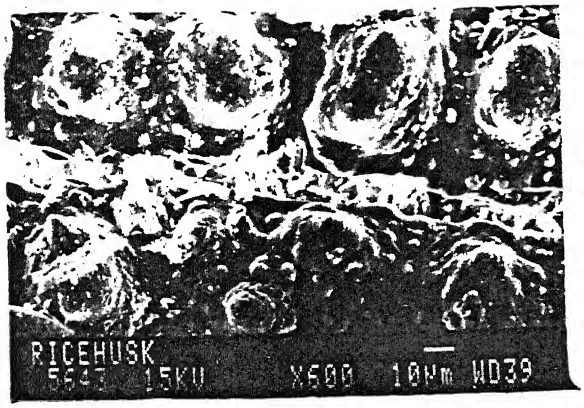

(c)

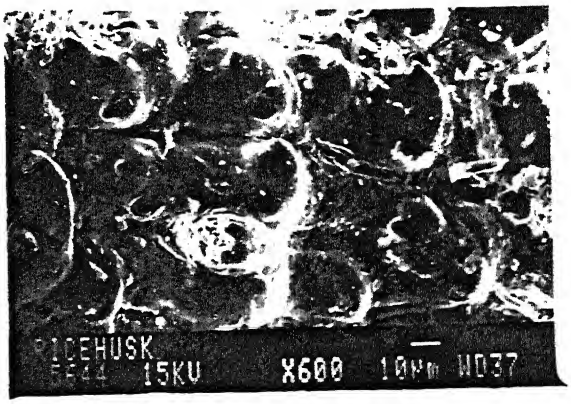

(d)

Figure 4.7: Scanning electron micrograph of rice husk ash produced in air at (a) 400°C, (b) 600°C, (c) 750°C and (d) 900°C, magnified 600 times.

4.2 Rice Husk Ash Produced Under Hydrogen Atmosphere

The rice husk char produced under hydrogen atmosphere were characterized for structure, surface area and chemical activity similar to rice husk ash produced in air. The results of these studies are presented below.

4.2.1 X-Ray Diffraction

X-ray diffraction pattern of all the samples [Fig-(4.8)] show a single hump indicating disordered structure. The shape of these humps are almost alike in all the cases despite samples prepared at different temperatures. It seems that X-ray diffraction is mainly due to amorphous silica particles. The intervining carbon atoms seems to contribute very little with respect to scattering from silica.

4.2.2 BET (Surface Area and Pore Volume)

The surface area and pore volume of all the samples prepared at different temperatures were determined from nitrogen adsorption at liquid nitrogen temperature.

Table 4.4: Surface area and pore volume of rice husk ash produced in hydrogen atmosphere

Husk Burning Temp.($^{\circ}C$)	Surface Area (m^2/gm)	Pore Volume (ml/gm)
400	6.29	0.0671*
600	49.41	0.0849*
750	70.76	0.0955
900	118.62	0.1181

[* Determined by liquid (acetone, ρ =0.8 gm/cm^3) impregnation technique.]

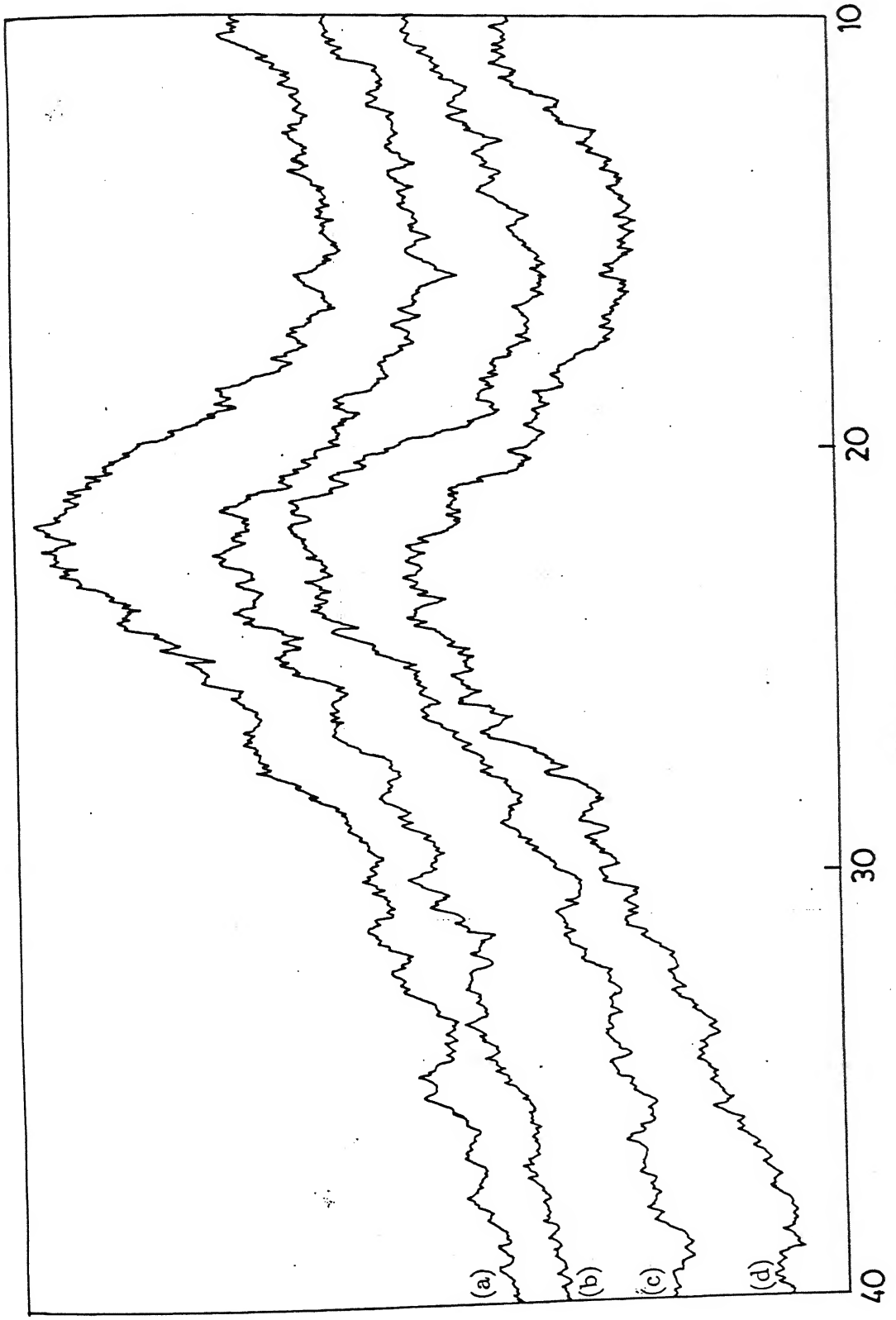

Figure 4.8: X-ray diffraction pattern of rice husk ash produced in hydrogen atmosphere at (a) 400°C, (b) 600°C, (c) 750°C and (d) 900°C.

From Fig-(4.9), it is evident that the specific surface area increases with charring temperature.

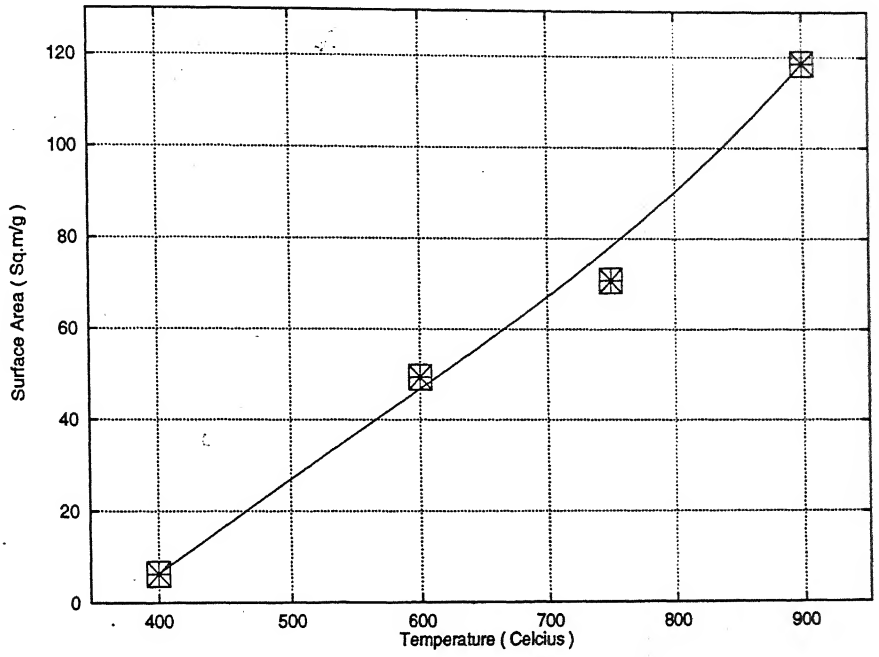

Figure 4.9: Variation of surface area with temperature of rice husk ash produced in hydrogen atmosphere.

The pore volume shows similar trend [Fig-(4.10)] i.e it increases with increasing temperature of char formation. This result is in distinct contrast to rice husk ash prepared in air, in which surface area decreases and pore volume increases with increasing temperature of ash formation.

In the present case, it seems that isolated pores result due to continuously increasing dissociation of hydrocarbon of silica matrix. This leads to increasing number of pores with increasing temperature. The pore volume therefore also increases with increasing number of pores of larger radii, as evident from comparison of pore diameter-pore volume distribution [Table-(4.5)] of the samples prepared at $750°C$ and $900°C$ respectively.

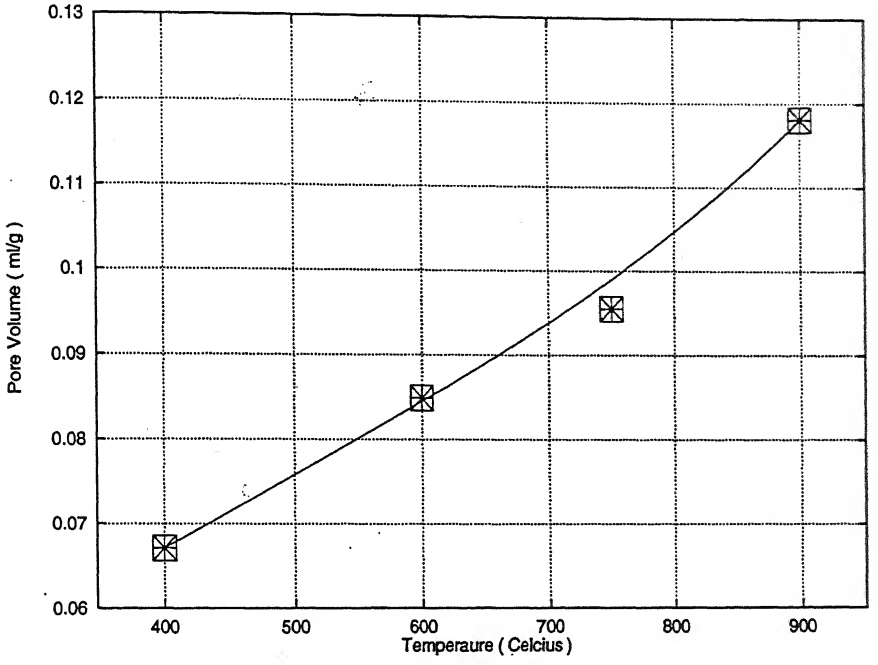

Figure 4.10: Variation of pore volume with temperature of rice husk ash produced in hydrogen atmosphere.

Table 4.5: Pore diameter and pore volume of rice husk ash produced in hydrogen atmosphere at $750°C$ and $900°C$

Pore Diameter Range (nm)	Pore Volume (ml/gm) [$750°C$]	Pore Volume (ml/gm) [$900°C$]
Under 6	0.01975 (31.87%)	0.01101 (15.06%)
6-8	0.00672 (10.85%)	0.00398 (5.45%)
8-10	0.00380 (6.14%)	0.00273 (3.74%)
10-12	0.00341 (5.50%)	0.00314 (4.29%)
12-16	0.00358 (5.78%)	0.00450 (6.16%)
16-20	0.00334 (5.39%)	0.00585 (8.00%)
20-80	0.01532 (24.73%)	0.03495 (47.81%)
Over 80	0.00604 (9.74%)	0.00694 (9.49%)

4.2.3 Energy of Activation

Table 4.6: lnA values of rice husk ash produced in hydrogen atmosphere

T (°C)	T (K)	1/T×10^3 K^{-1}	A	Ȧ=A/3600	lnȦ
400	673	1.485	6.29	0.0017	-6.377
600	873	1.145	49.41	0.0137	-4.288
750	1023	0.977	70.76	0.0196	-3.929
900	1173	0.852	118.62	0.0329	-3.412

Variation of lnȦ with 1/T is shown in Fig-(4.11). From the figure, slope is found to be -4.68×$10^3$and the corresponding value of $\triangle E_a$ is 38.91 kJ/mol. The positive sign of $\triangle E_a$ suggests the process to be endothermic. This is in contrast to the process taking place in air, where it is exothermic.

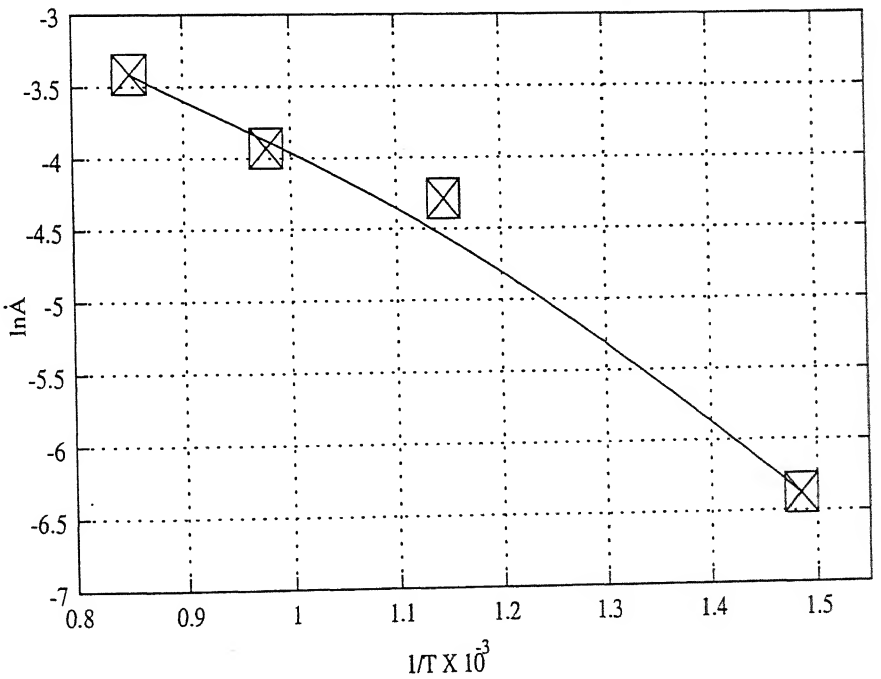

Figure 4.11: Variation of lnȦ with 1/T of rice husk ash produced in hydrogen atmosphere.

4.2.4 Elemental Analysis

The samples prepared were analyzed for the presence of silicon, potassium, calcium and iron. The relative weight percent of these elements is given in the Table-(4.7) below.

Table 4.7: Weight percent of silicon, potassium, calcium and iron in rice husk ash produced in hydrogen atmosphere

Husk Burning Temp. (°C)	Si (wt.%)	K (wt.%)	Ca (wt.%)	Fe (wt.%)
400	48.75	28.41	18.65	4.18
600	69.62	16.00	10.30	4.08
750	71.57	18.57	9.83	0.00
900	91.95	6.72	1.33	0.00

From the Fig-(4.12), the relative weight percent of silicon increases, while that of other three [Fig-(4.13)] decreases.

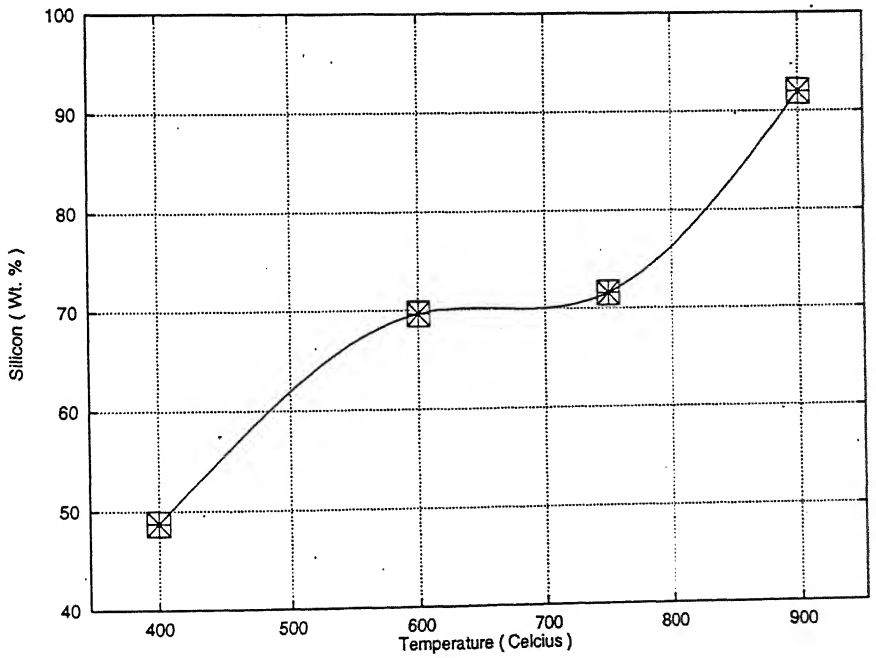

Figure 4.12: Variation of weight percent of silicon with temperature in rice husk ash produced in hydrogen atmosphere.

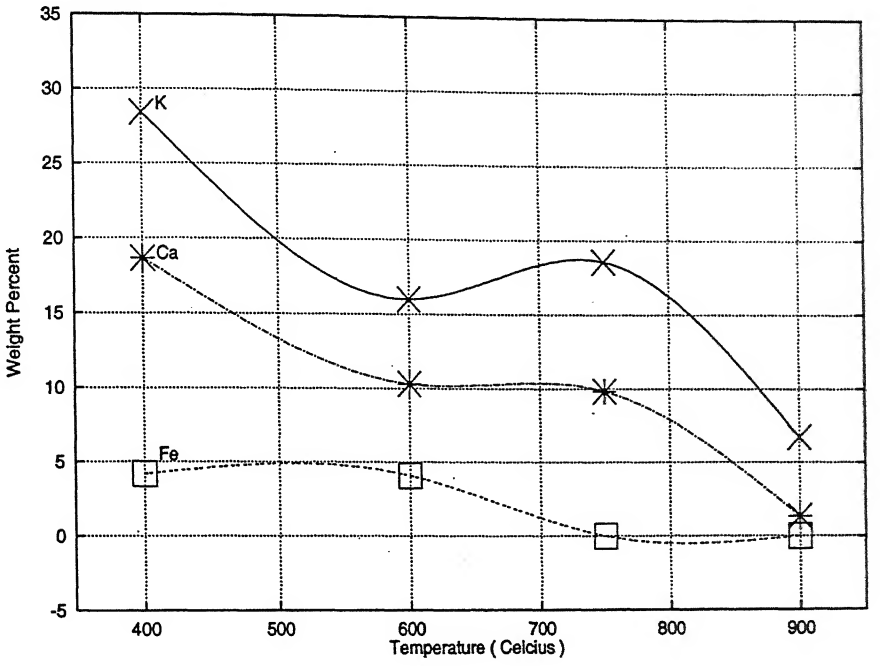

Figure 4.13: Variation of weight percent of potassium, calcium and iron with temperature in rice husk ash produced in hydrogen atmosphere.

It seems that potassium, calcium and iron are present in some oxide form or as hydrated salts, which sublimates at increasing process temperature. It may be that potassium, calcium and iron all are in some complex form or forms complex under process condition, which on increasing process temperature comes out of the silica matrix leading to apparent enhancement of silicon percent.

4.2.5 SEM Microstructure

Topographic scanning electron micrographs for samples prepared at various temperatures are shown in Fig-(4.14). As the processing temperature increases, some kind of progressive smoothening seems to result. As extensive lattice diffusion could result into significant decrease in specific surface area , such a possibility is discounted. Chemical leaching of carbon due to hydrogen therefore may be one of the possible causes of progressive topographic smoothening.

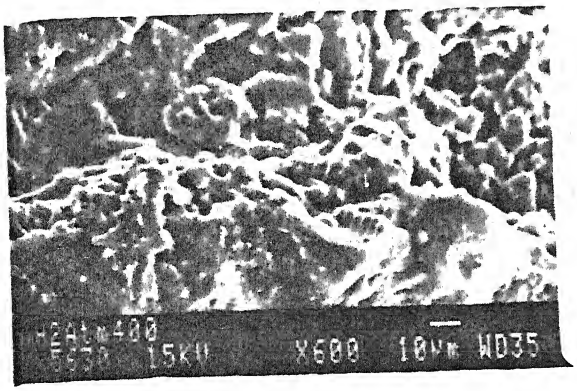

(a)

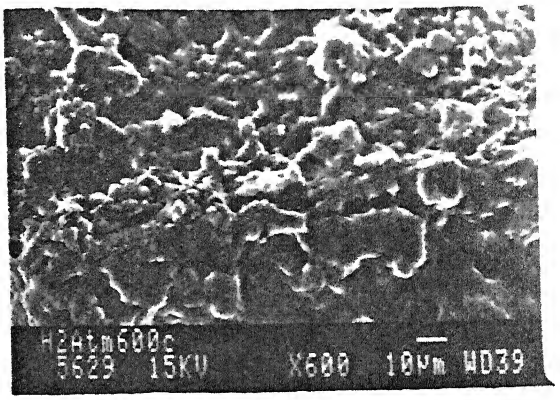

(b)

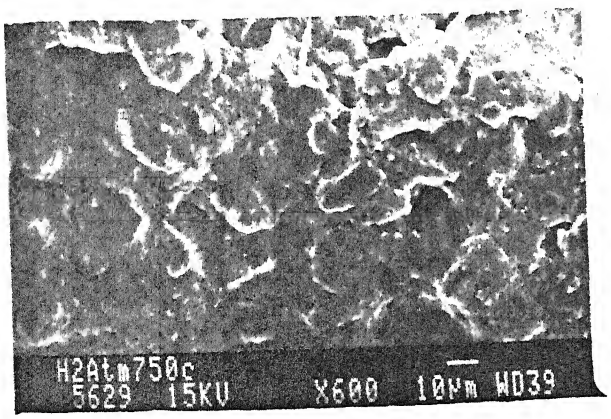

(c)

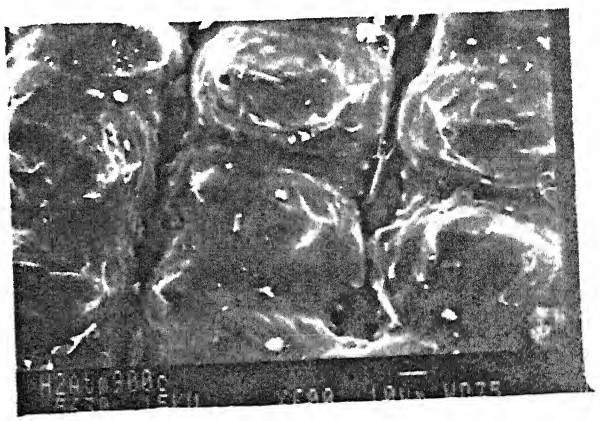

(d)

Figure 4.14: Scanning electron micrograph of rice husk ash produced in hydrogen atmosphere at (a) 400°C, (b) 600°C, (c) 750°C and (d) 900°C, magnified 600 times.

4.3 Activated Rice Husk Ash

The results of the rice husk char produced at 350°C followed by activation of the above char with 20% H_3PO_4 and heating at various temperature (600°C to 1000°C) are given below.

4.3.1 X-Ray Diffraction

X-ray diffraction pattern of all the samples prepared at 600, 700, 800 and 900°C shows no peaks [Fig-(4.15)], indicating them to be amorphous. In all cases, a hump is observed in the 2θ range of 16 to 39. However, in the XRD pattern of sample prepared at 1000°C [Fig-(4.16)] well defined peaks were found. These peaks have been assigned to calcium phosphate silicate ($Ca_7Si_2P_2O_{16}$) formation.

4.3.2 Surface Area

Surface area of all the samples prepared at different temperatures are given in the Table-(4.8) below.

Table 4.8: Surface area and ln$\dot{A}$ values of activated husk ash

T (°C)	T (K)	1/T×10^3 K^{-1}	A	$\dot{A}$=A/(4×3600)	ln$\dot{A}$
600	873	1.145	11.25	0.0008	-7.155
700	973	1.028	14.41	0.0010	-6.907
800	1073	0.932	111.79	0.0078	-4.858
900	1173	0.852	76.49	0.0053	-5.238
1000	1273	0.785	1.34	0.0001	-9.282

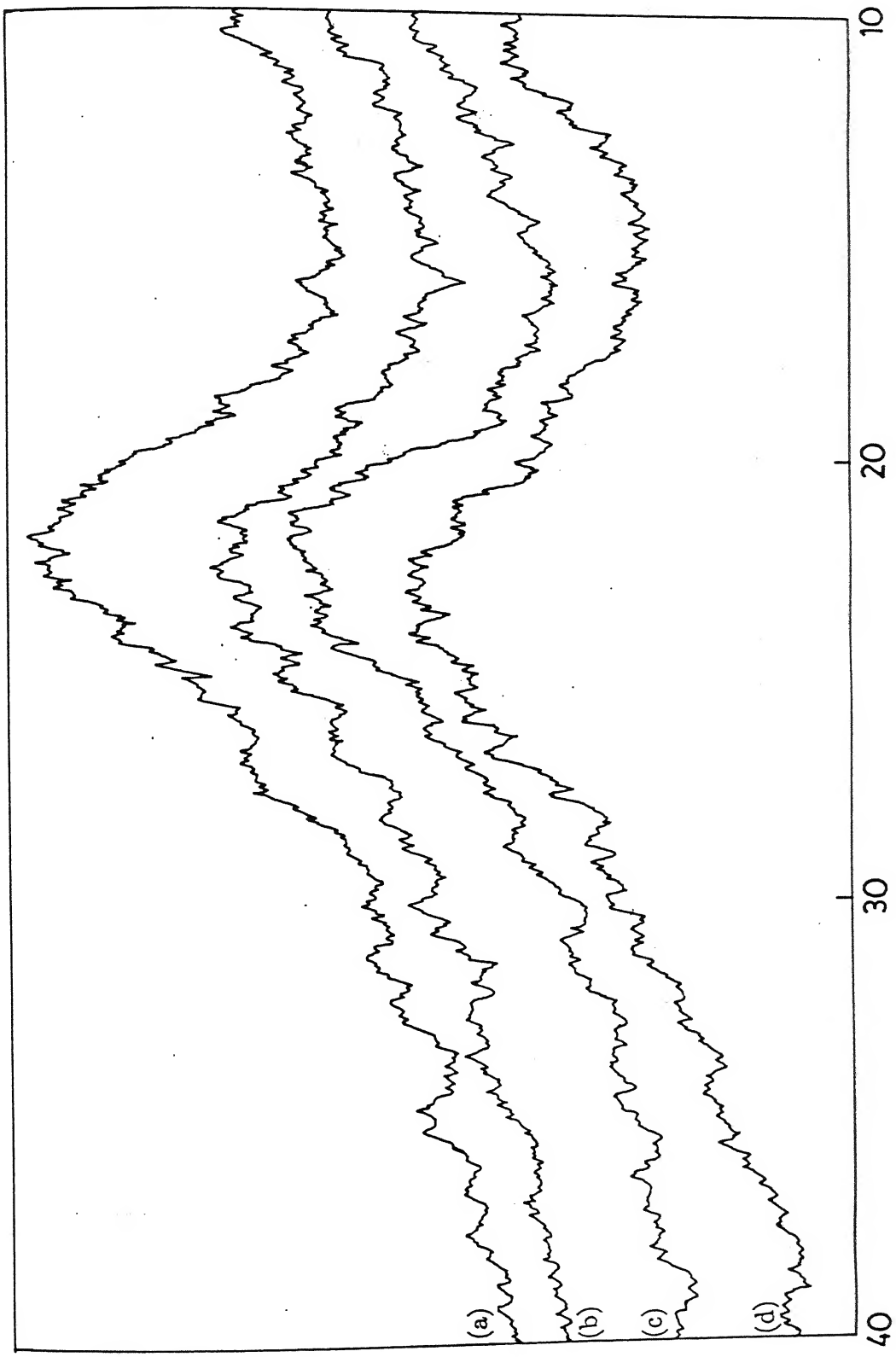

Figure 4.15: X-ray diffraction pattern of activated husk ash produced at (a) 600°C, (b) 700°C, (c) 800°C and (d) 900°C.

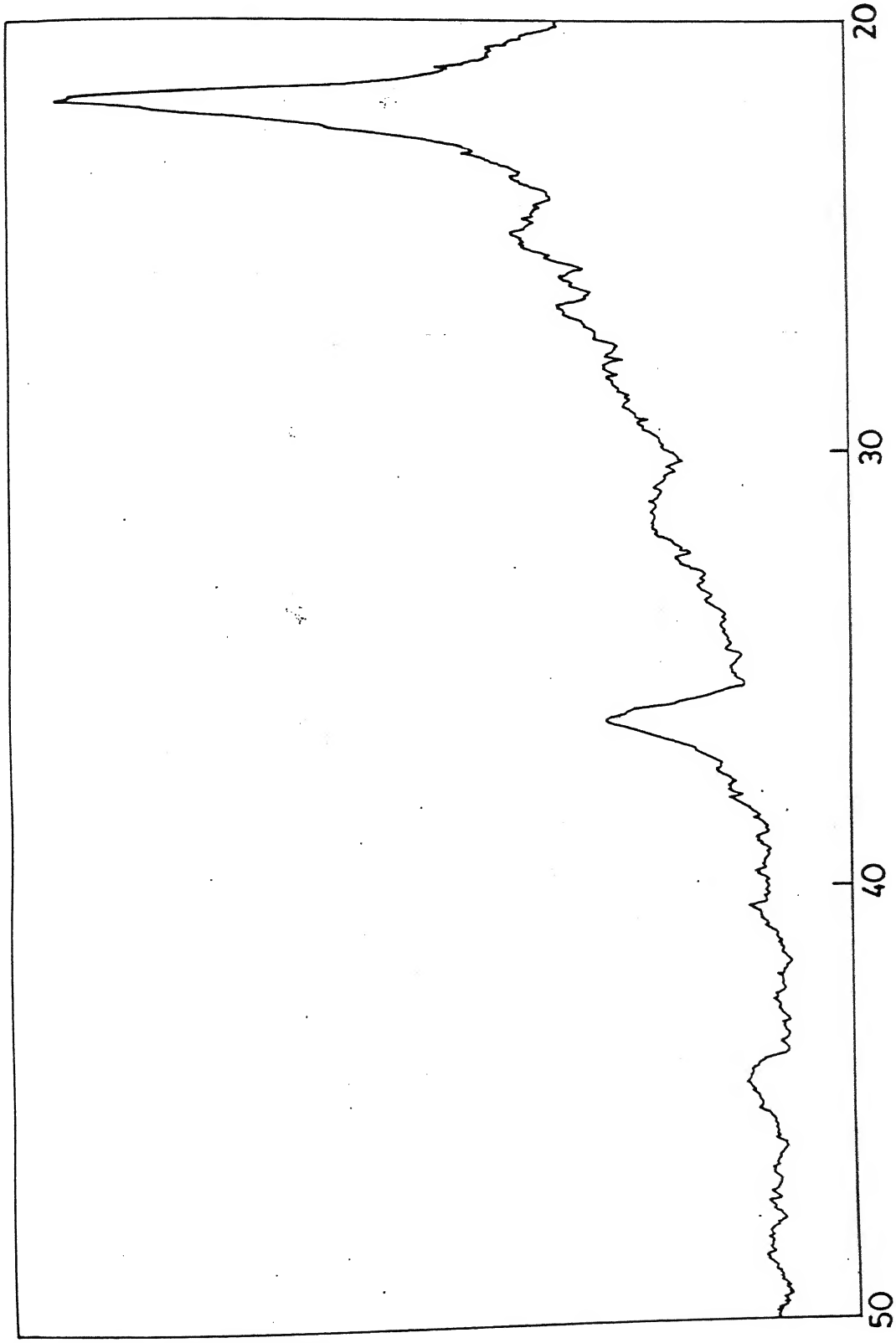

Figure 4.16: X-ray diffraction pattern of activated husk ash produced at 1000°C.

From Fig-(4.17), it is interesting to note that surface area is very small at 600°C and 700°C. This is due to the absorption of H_3PO_4 in the pores. However, as the temperature increases, the evaporation of H_3PO_4 from the pores starts taking place and surface area starts increasing with increasing temperature. Beyond 800°C, especially at 1000°C, surface area starts decreasing drastically, possibly due to chemical reactions involving SiO_2, K_2O and CaO. This is also suggested by the X-ray diffraction pattern of the samples, which used to give a single hump upto 900°C, started showing well defined peaks at 1000°C. This confirms the interaction between substrate and H_3PO_4.

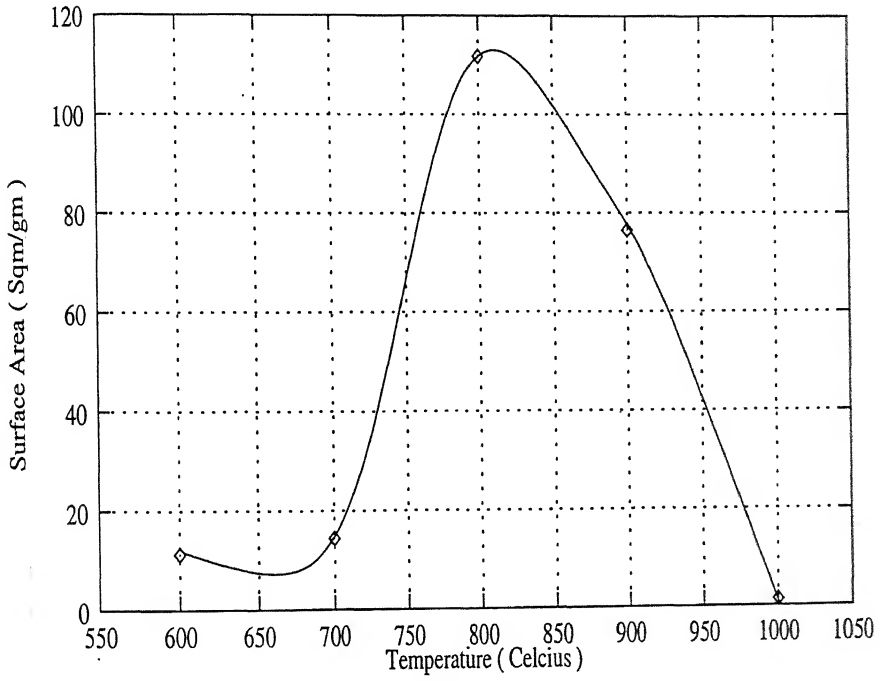

Figure 4.17: Variation of surface area with temperature of activated husk ash.

4.3.3 Energy of Activation

The variation of lnÂ with 1/T is shown in Fig.-(4.18). From the figure, value of slope at lower and higher temperature is found to be -2.12×10^3 and 60.36×10^3repectively and the corresponding values of $\triangle E_a$ are 17.63 kJ/mol and -501.82 kJ/mol. The sign of $\triangle E_a$

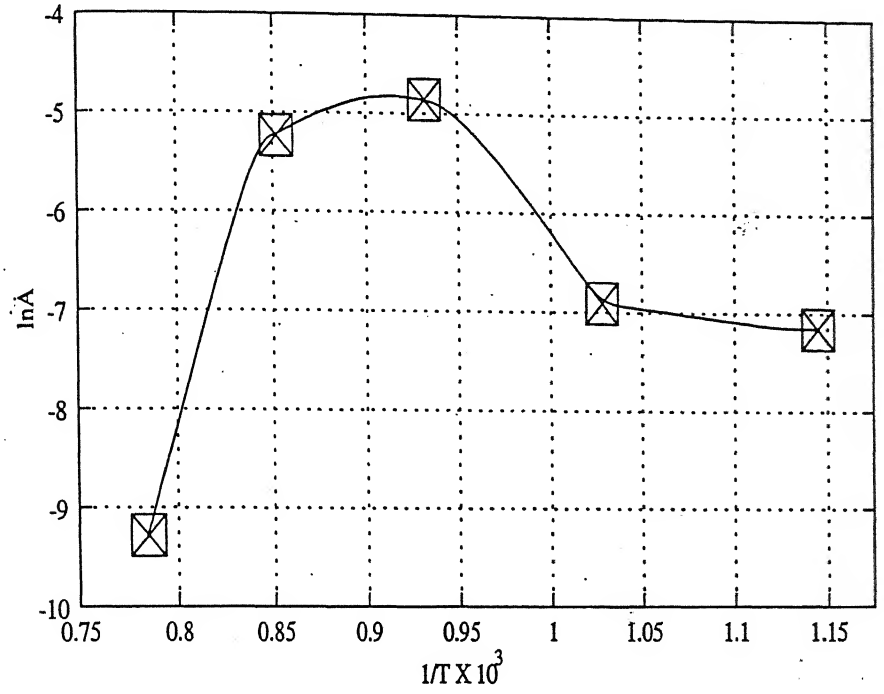

Figure 4.18: Variation of $\ln\hat{A}$ with 1/T of activated husk ash

suggests that the process is endothermic at lower temperature and becomes exothermic at higher temperature. This may be possibly due to change in mechanism during charring or due to some other chemical reactions, which starts taking place at higher temperature.

4.3.4 SEM Microstructure

The scanning micrographs of all the samples are shown in Fig-(4.19) and Fig-(4.20), also reveals gradual microstructural changes specially at high temperatures (900°C and 1000°C). Microstructure which reveals very rough features at low temperatures slowly becomes smoother with sharp edged cavities, possibly due to thermally activated chemical reaction.

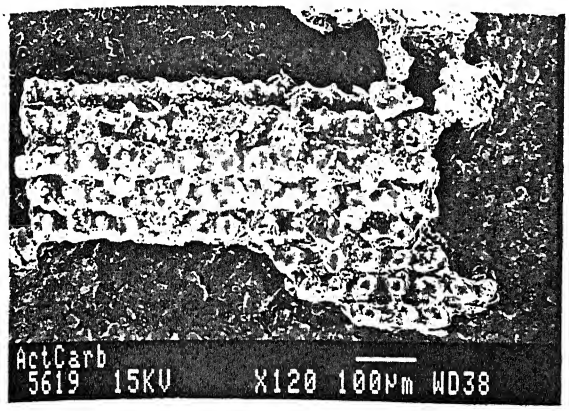

(a)

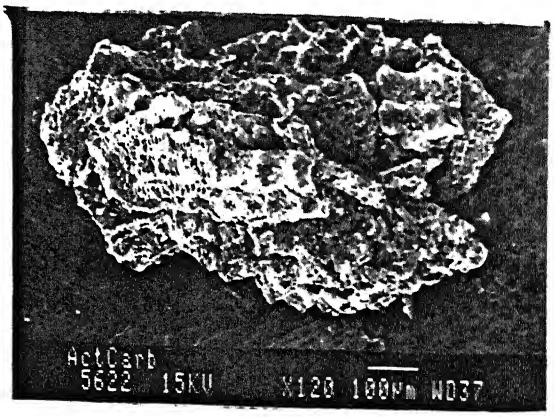

(b)

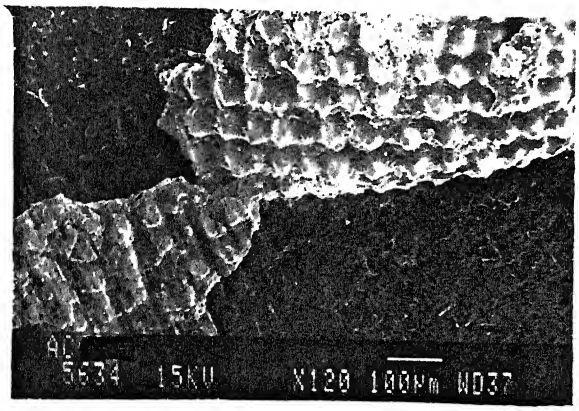

(c)

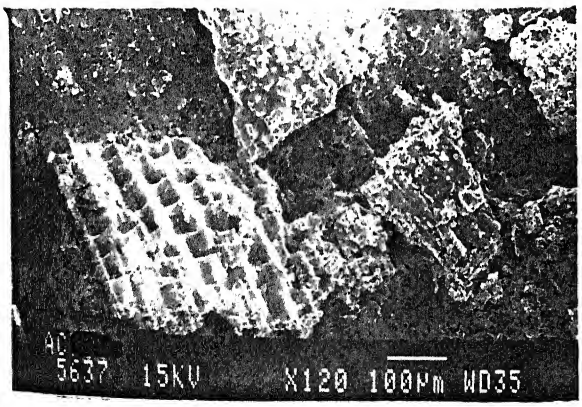

(d)

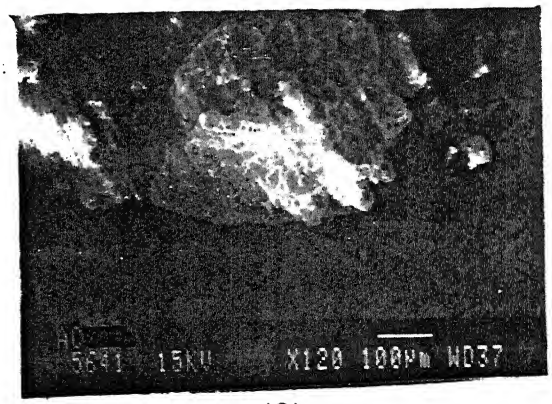

(e)

Figure 4.19: Scanning electron micrograph of activated husk ash produced at (a) 600°C, (b) 700°C, (c) 800°C, (d) 900°C and (e) 1000°C, magnified 120 times.

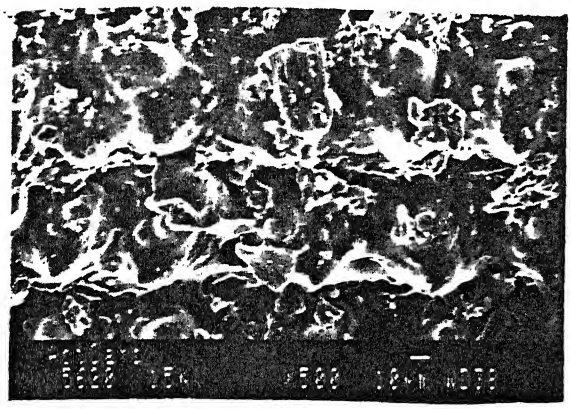

(a)

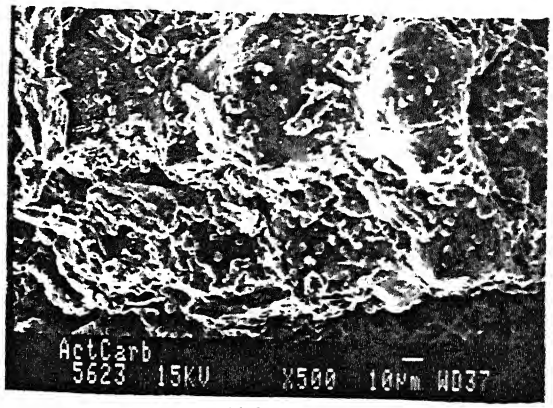

(b)

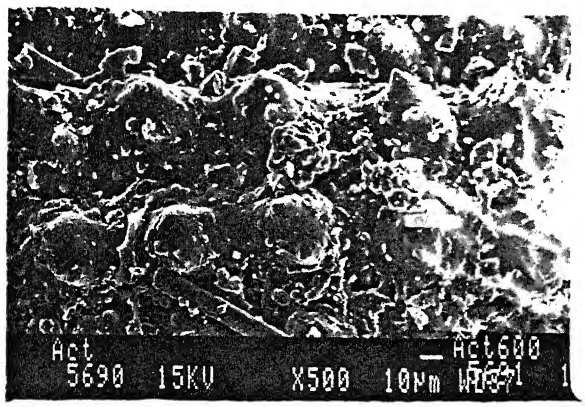

(c)

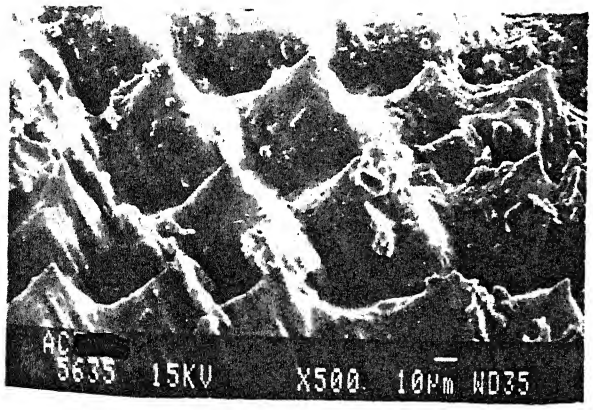

(d)

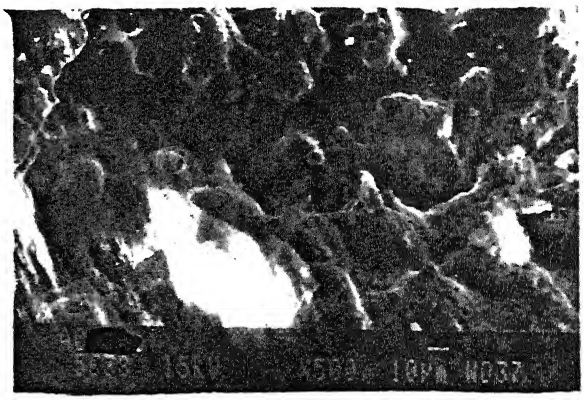

(e)

Figure 4.20: Scanning electron micrograph of activated husk ash produced at (a) 600°C, (b) 700°C, (c) 800°C, (d) 900°C and (e) 1000°C, magnified 500 times.

4.4 Chemical Activity Test

Chemical activity was determined by molasses test and iodine test. The results of these tests are given below separately.

4.4.1 Molasses test

The results of molasses test as prescribed by [84] for decolorization is presented in the Table-(4.9) for all the three kinds of materials prepared. The values within bracket indicates the relative difference between the data obtained from materials prepared in the present investigation and that from standard activated carbon.

Table 4.9: Percent decolorization of molasses solution by different husk ash

Amount (gm)	Activated Husk	Air Charred	Hydrogen Charred
0.1	55	50	45
0.3	65 (+3)	60 (-2)	55 (-7)
0.5	80 (0)	70 (-10)	65 (-15)

The variation of percent decolorization of molasses solution with the amount of samples, for all the three materials are shown in Fig-(4.21). It is evident that percent decolorization of molasses solution increases with the amount of sample in all cases. The variation is linear for the samples prepared in air and hydrogen. However, the activated husk sample shows mild curvature towards decolorization axis showing better efficiency with increasing amount. Slope of the lines (curves) in all the three cases are nearly same indicating identical adsorption mechanism. The decolorization curves for different materials lies one over another. This indicates that activated husk has maximum activity and hydrogen charred husk has minimum activity.

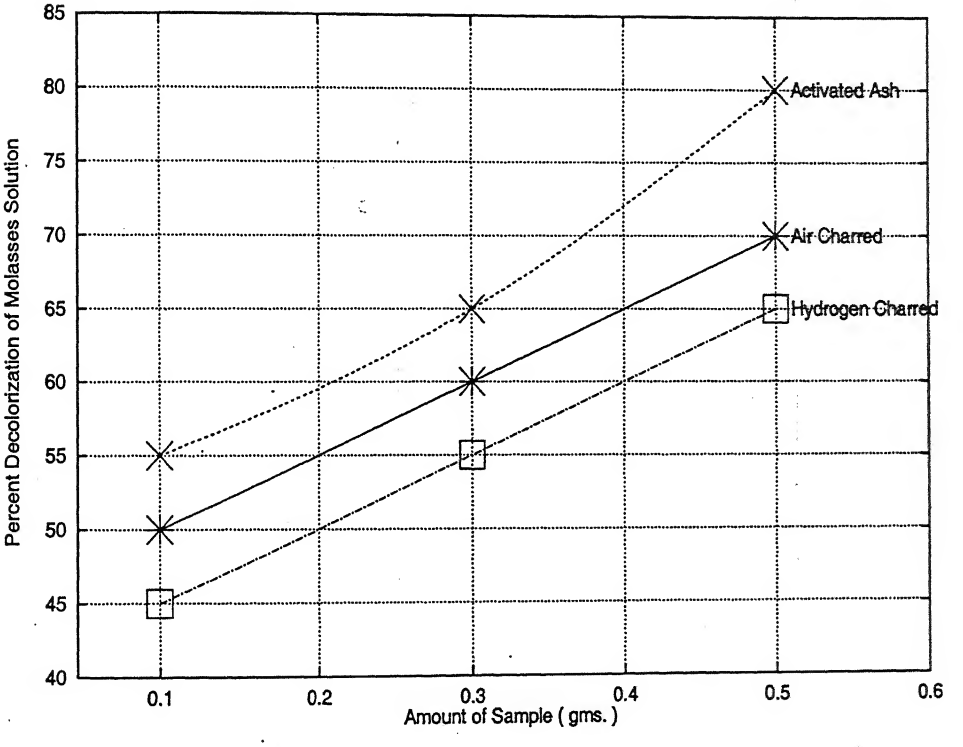

Figure 4.21: Variation of percent decolorization of molasses solution with amount of samples.

4.4.2 Iodine Test

The iodine decolorization tests for all the three materials are shown in Table-(4.10) and the corresponding graphical presentation is shown in Fig-(4.22).

Table 4.10: Percent decolorization of iodine solution by different husk ash

Amount (gm)	Activated Husk	Air Charred	Hydrogen Charred
0.1	50	45	40
0.3	55 (-7)	50 (-12)	45 (-17)
0.5	65 (-15)	55 (-25)	50 (-30)

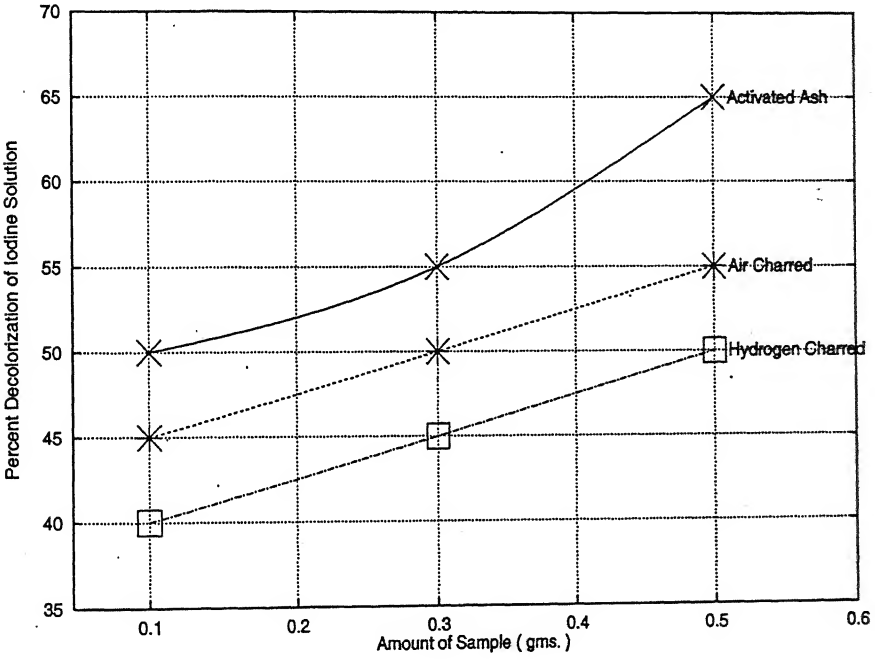

Figure 4.22: Variation of percent decolorization of iodine solution with amount of samples.

Decolorization in the present case is quite similar to that of molasses test. However, percent activity in this case is certainly smaller in comparison to molasses test. Values in bracket shows the difference between present activity and standard activated carbon[84].

4.4.3 Effect of Time

The time dependent color adsorption of molasses solution was studied by 0.5 gm and 0.3 gm of activated husk ash. The results of these observation are given in Table-(4.11) below.

Table 4.11: Percent decolorization of molasses solution with time

Time (minutes)	For 0.5 gm.	For 0.3 gm.
10	70	55
20	75	60
30	80	65
40	80	65

From Fig-(4.23), it is evident that as the reaction time increases, the percent decolorization of molasses solution increases and reaches to equilibrium after 30 minutes.

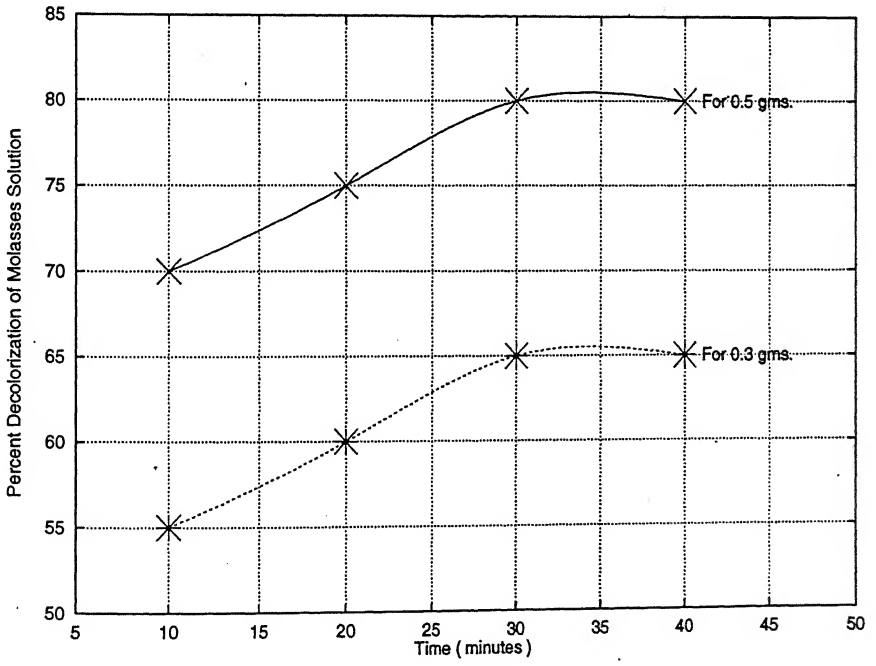

Figure 4.23: Variation of percent decolorization of molasses solution with time

Chapter 5

Conclusions

1.Following three different categories of rice husk ash have been prepared and characterized.

(i) Ash prepared by firing rice husk in air,

(ii) Ash prepared by firing rice husk in hydrogen atmosphere and

(iii) Air fired ash activated with phosphoric acid.

2. Ash prepared in air and hydrogen atmosphere exhibited amorphous structure upto $900°C$. However, phosphoric acid activated ash showed transition from amorphous to crystalline structure, due to the formation of calcium phosphate silicate at $1000°C$.

3. Specific surface area was found to increase continuously with firing temperature in the case of ash prepared under hydrogen atmosphere. However, specific surface area of air fired ash was found to decrease with increasing firing temperature. The behavior of activated ash was found to be different in comparison to above two. The specific area first increased with processing temperature till around $800°C$ and then started decreasing fast with temperature.

4. Chemical activity of decolorizing molasses and iodine solution by these products can be kept in order of decreasing activity as, activated ash > air fired ash > hydrogenated ash.

Appendix

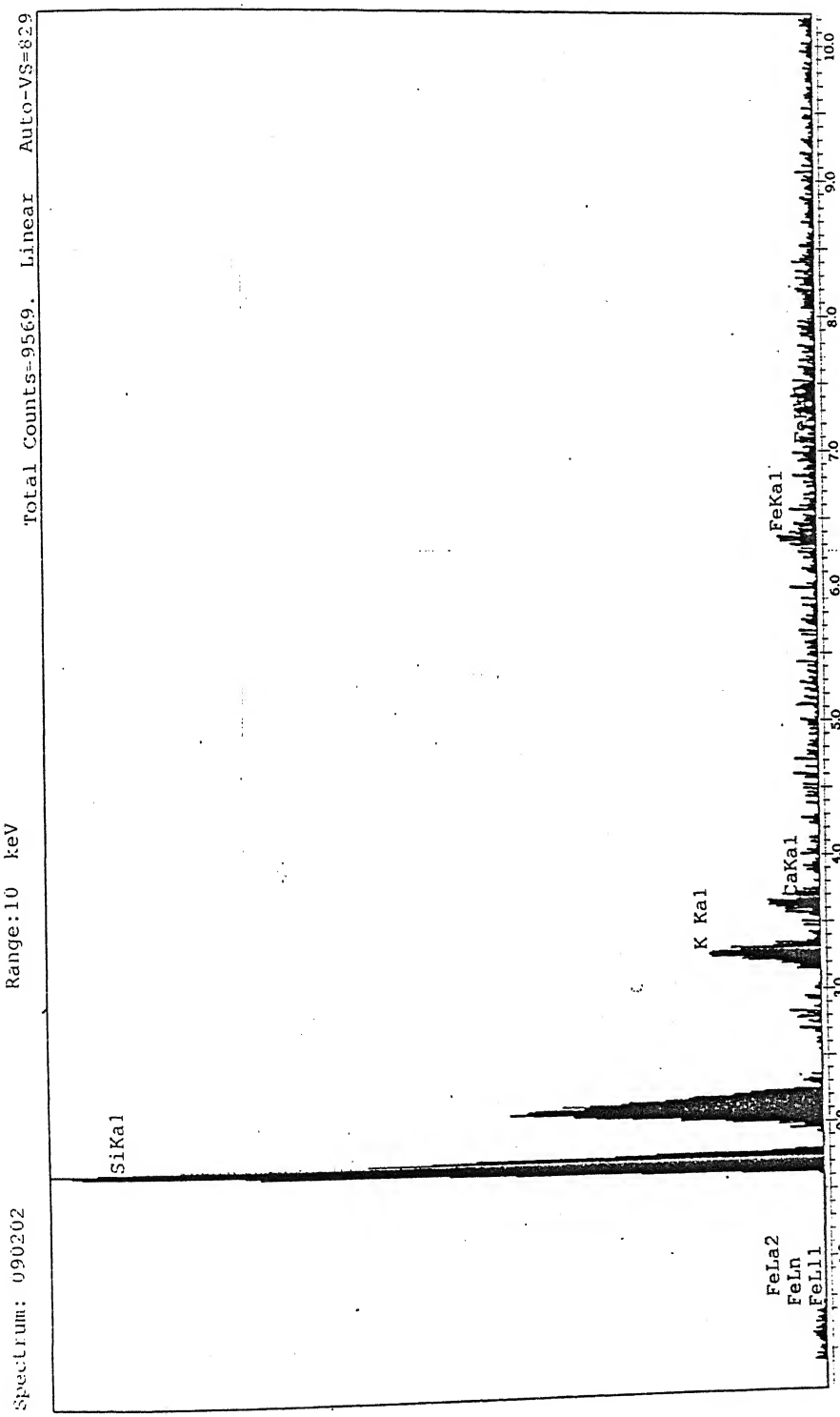

Figure A.1: Energy Dispersive Spectra of rice husk ash produced in air at 400°C

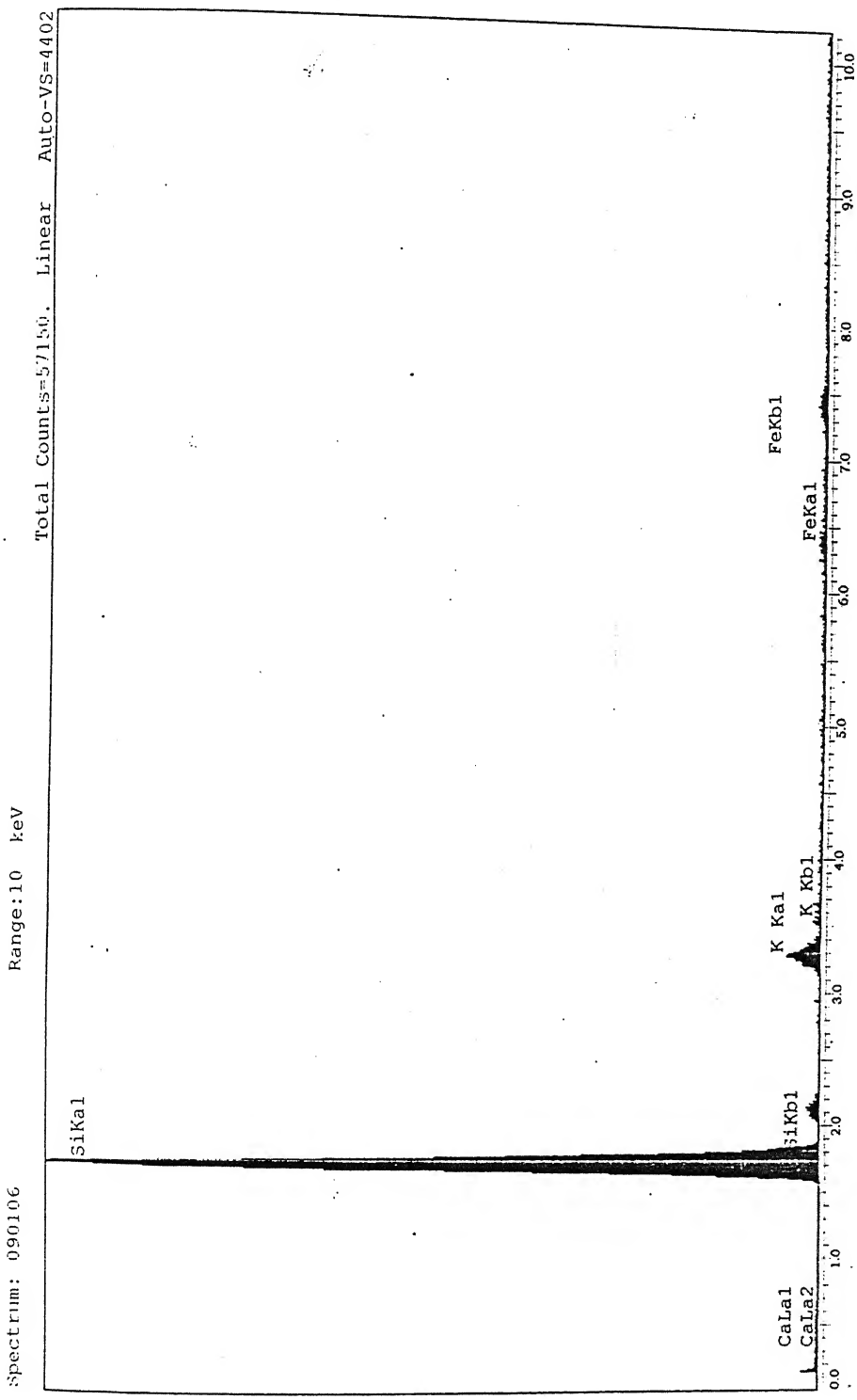

Figure A.2: Energy Dispersive Spectra of rice husk ash produced in air at 600°C

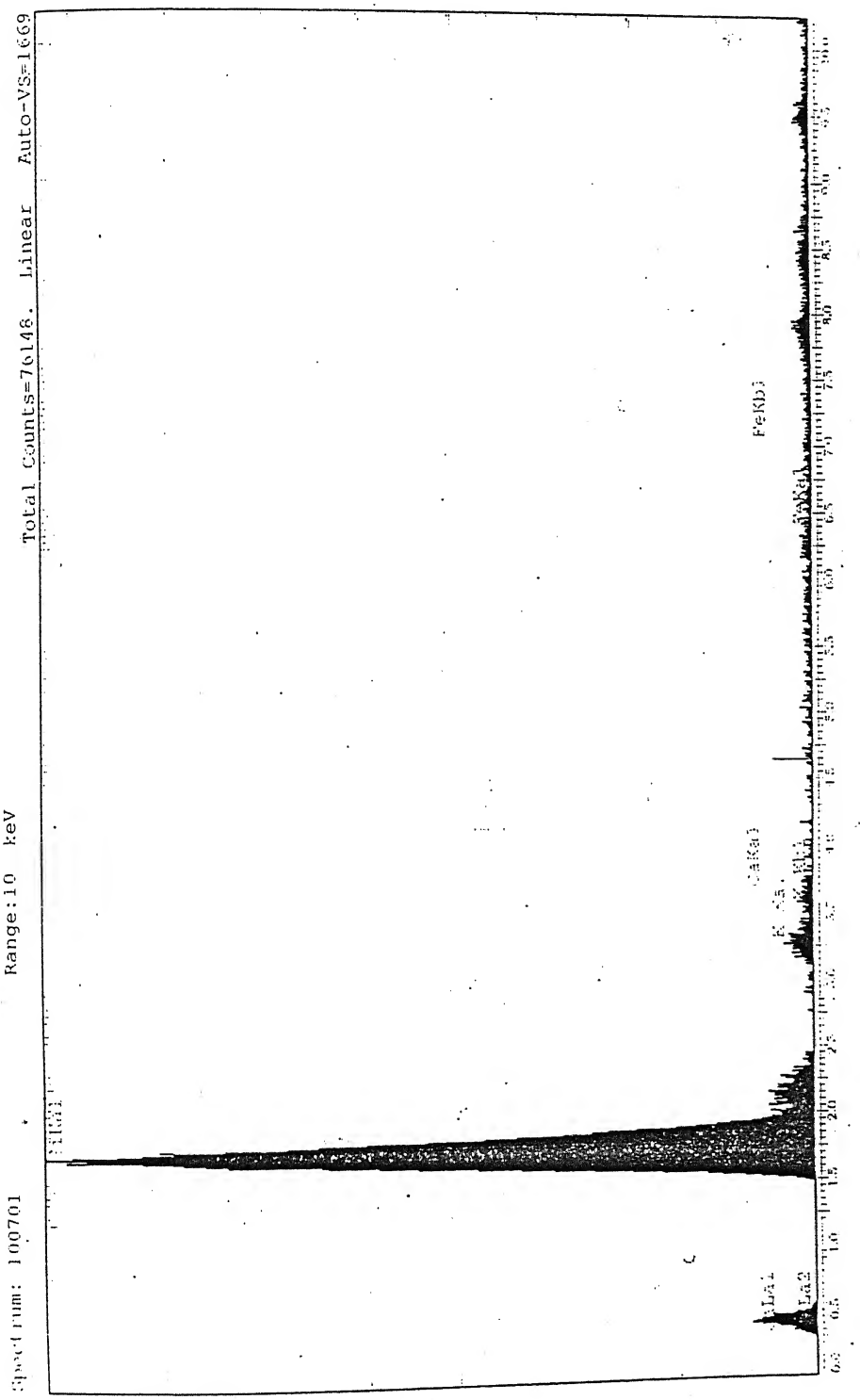

Figure A.3: Energy Dispersive Spectra of rice husk ash produced in air at 750°C

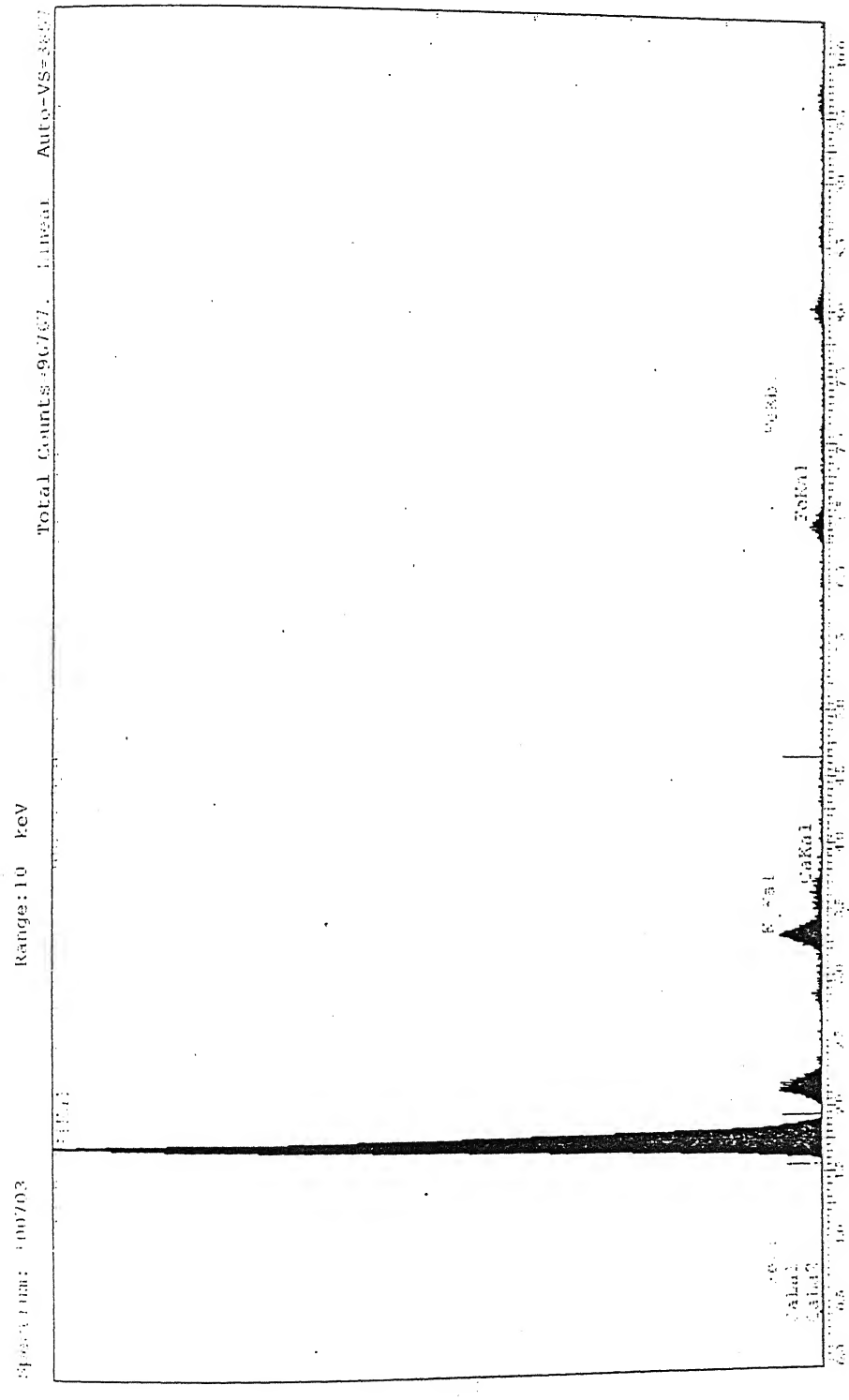

Figure A.4: Energy Dispersive Spectra of rice husk ash produced in air at 900°C

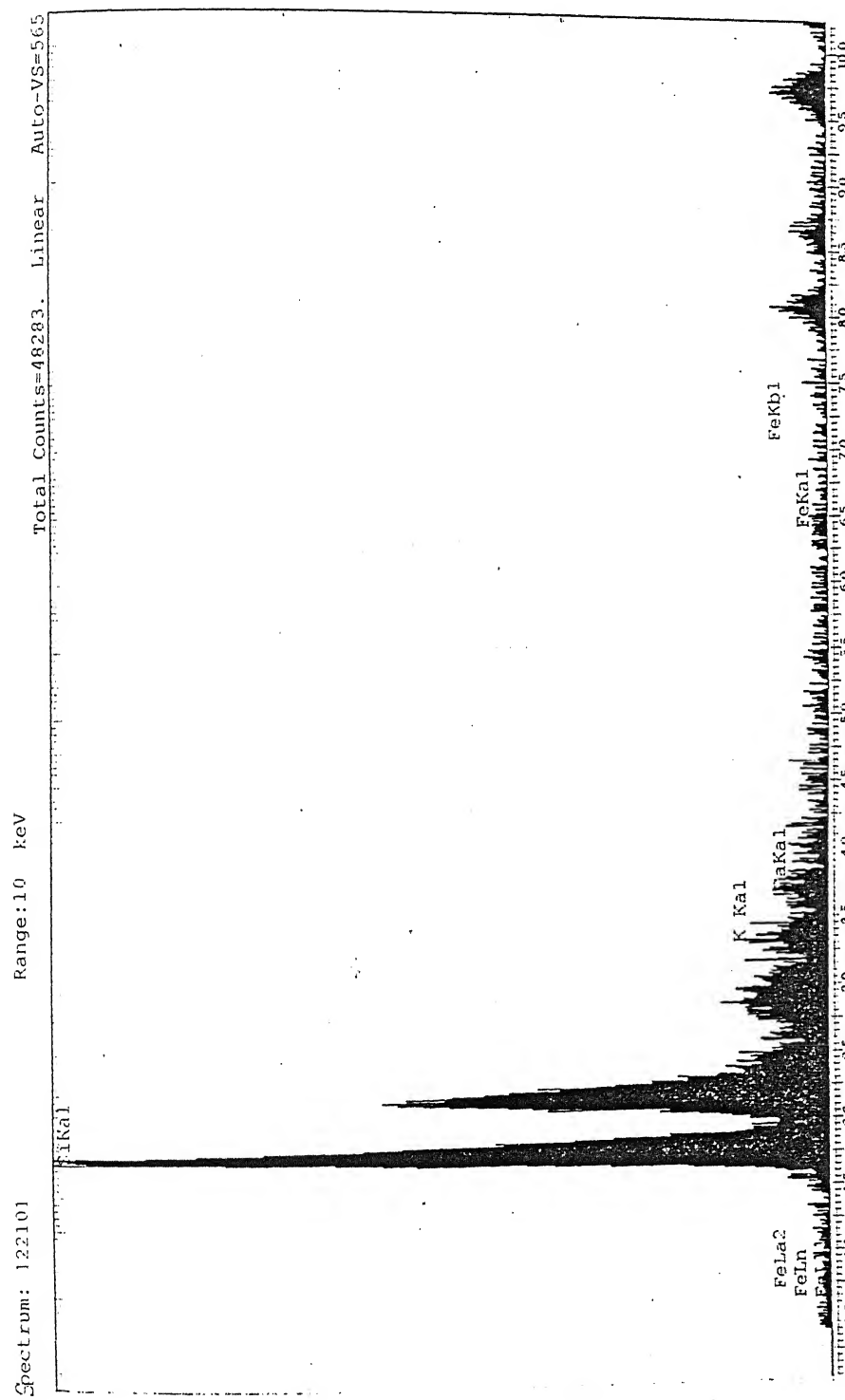

Figure A.5: Energy Dispersive Spectra of rice husk ash produced in hydrogen atmosphere at 400°C

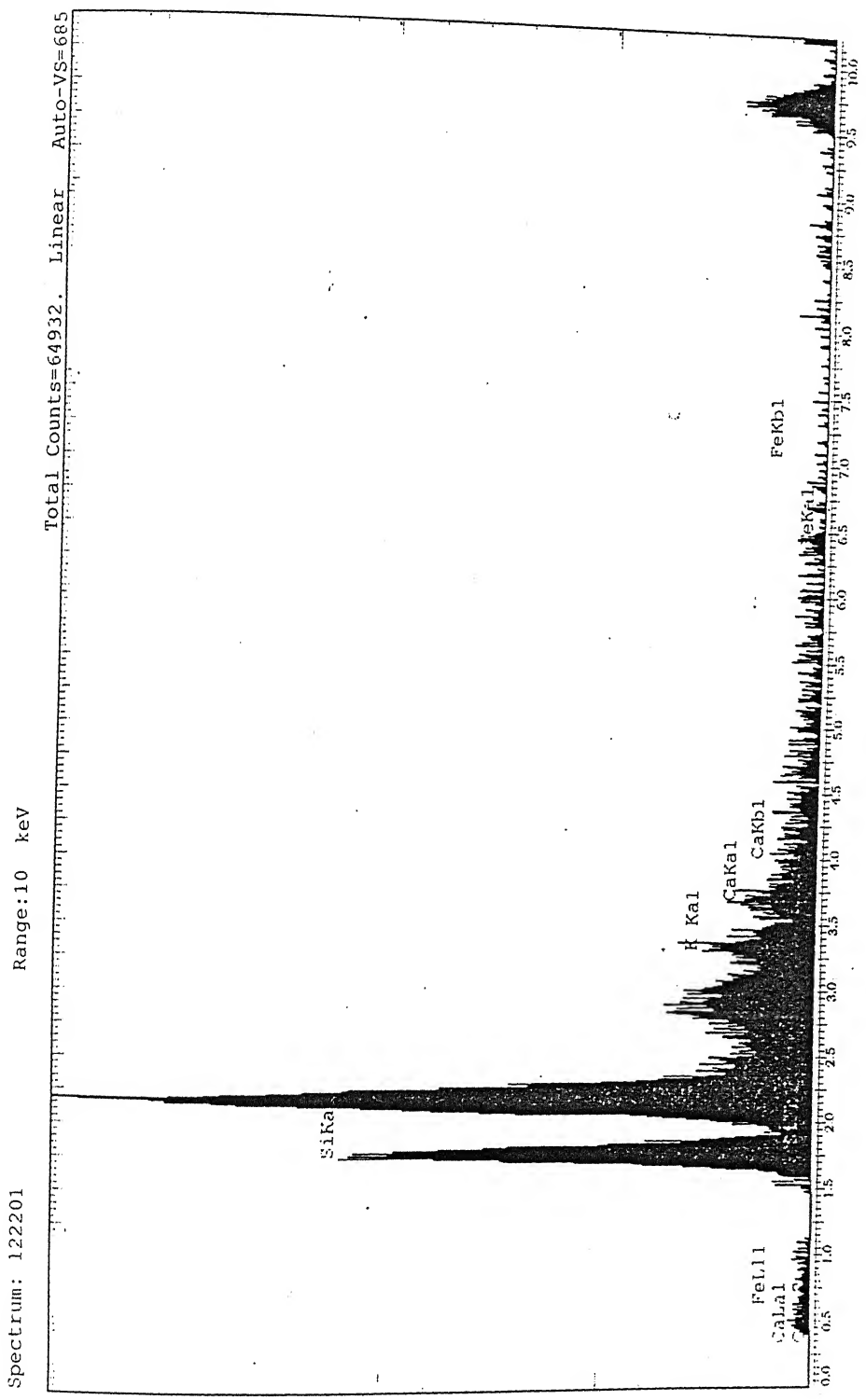

Figure A.6: Energy Dispersive Spectra of rice husk ash produced in hydrogen atmosphere at $600°C$

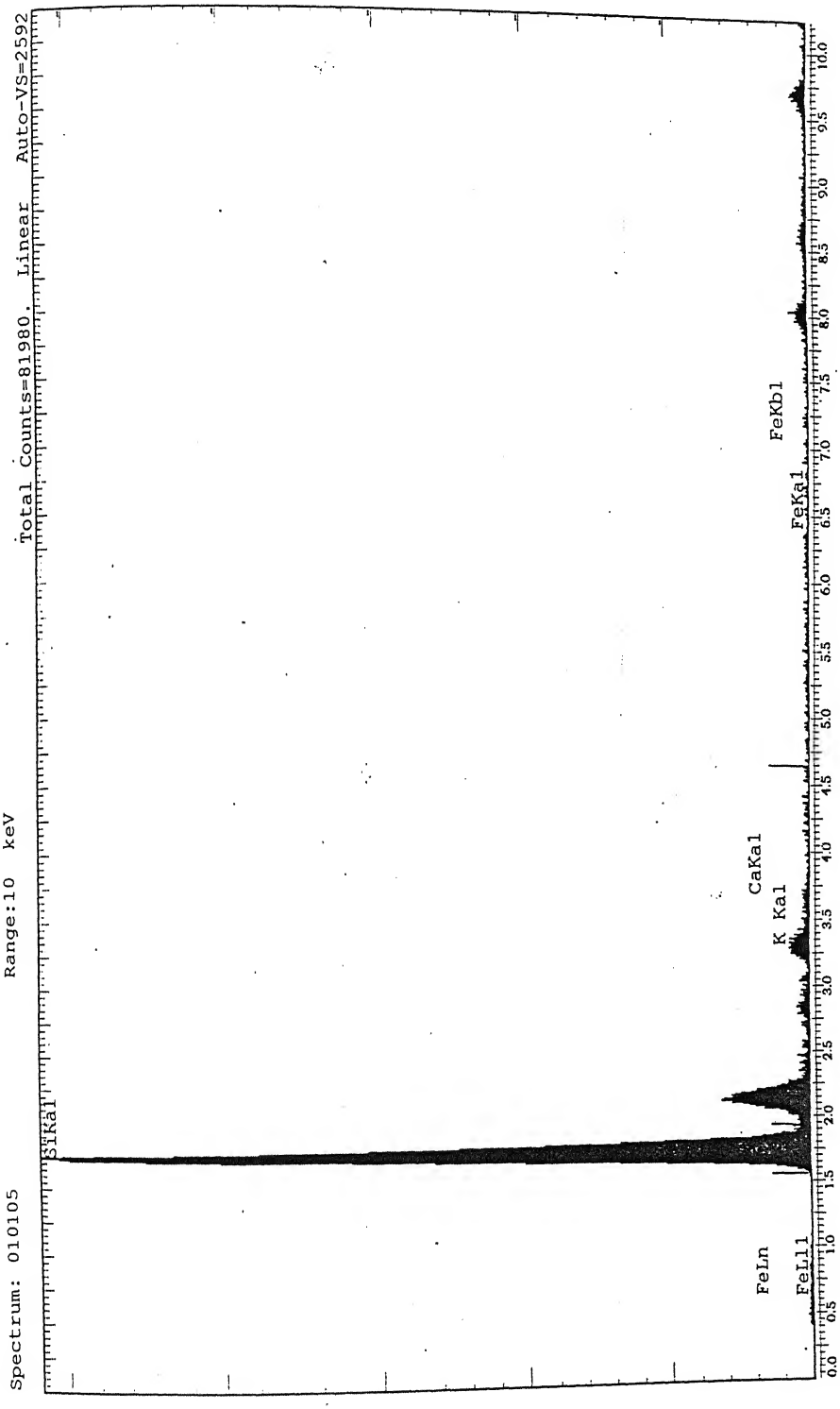

igure A.8: Energy Dispersive Spectra of rice husk ash produced in hydrogen atmosphere at 900°C

References

[1] Teng,H., Lin,H.C. and Ho,J.A.; Ind. Eng. Chem. Res., 1997, 36(9), 3974-977 (Eng.).

[2] Patel,M., Kumari,P. and Padhi,B.K.; Silic. India, 1992, 57(9-10), 155-9 (Eng.).

[3] Saprykin,L.V., Kiseleva,N.V. and Tamerdashev,Z.A.; Khim. Drev., 1989, (1), 107-9 (Russ.).

[4] Saprykin,L.V., Temerdasev,Z.A., Vasil'ev,A.M., Bregeda,I.D. and Masenko,B.P.; Khim. Drev., 1988, (6), 87-90 (Russ.).

[5] Ryu,S.E., Kim,T.N. and Kang.T.K.; J. Mater. Sci., 1997, 32(24), 6639-6643.

[6] Hayasi,Hisato and Nakashima,Satoru; Clay Sci., 1992, 8(4), 181-93.

[7] Yang Xianhe (Ministry of Communications, Research Inst. of Highway Science) Faming Zhuanli Shenging Gongkai Shuomingshu CN 1,063,087 (C1. CO1B 33/12), 29 July 1992, Appl. 92,100,466, 25 Jan 1992; 11 pp.

[8] Cook,C.B, Speare,P.R.S. and Tebbit,J.B (Kingsway Group PLC) PCT Int. Appl. WO 95 10,488 (C1 C04B 18/10), 20 Apr. 1995, GB Appl. 93/21, 359, 15 Oct. 1993; 22 pp.

[9] Communal,J.P., Fabre,F. and Mottot,Y.; Eau, Ind. Nuisances, 1996, 192, 35-38 (Fr.).

[10] Chakraverty,A. and Kaleemullah,S.; Energy Convess. Manage., 1991, 32(6), 565-70.

[11] Huang,Xiaoying, Faming Zhuanli Shenging Gongkai Shuomingshu CN 86,104,705 (C1. C01B 33/133), 18 May 1988, Appl. 14 July 1986; 8 pp.

[12] Rao,G.M., Sastry,A.R.K. and Rohatgi,P.K.; Bull. Mater. Sci., 1989, 12(5), 469-479.

[13] Ghosh,T.B., Nandi K.C., Acharya,H.N. and Mukherjee,D.; Mater. Lett., 1991, 12(3), 175-8.

[14] Eminov,A.M., Atakuziev,T.A. and Muslimov,B.A.; Steklo Keram, 1991, (11), 26-7 (Russ.).

[15] Basu,P.K., Roy,S.K., Das,J., Bhattacharjee,A. and Roy,S.K. (Council of Scientific and Industrial Research, India) Indian IN 168,399 (C1 B01J 29/04), 23 Mar. 1991, Appl. 87/DE990, 18 Nov. 1987; 15 pp.

[16] Didamony,H., Wahed,M.G., Elewa,K.M. and Amer,A.A.; Arab Gulf J. Sci. Res., A 1987, 5(1), 45-57 (Eng.).

[17] Fukazawa,M. (Tokai Carbon Kk) Jpn. Kokai Tokkyo Koho Jp 07,149,921 [95,149,921] (C1. C08J 5/14), 13 Jun 1995, Appl. 93/325,961, 30 Nov. 1993 ; 6 pp.

[18] Komatsu,M., Adachi,Y., Maeda,E., Nakamizo,M. and Sudo,K.; Kyushu Kogyo Gijutsu Kenkyusho Hokoku 1995, 54, 3395-9 (Japan).

[19] Yoshikawa,S. (Tokai Carbo Kk,Japan) Jpn. Kokai Tokkyo Koho Jp 08 26,848 [96,26,] (C1 C04B 38/06), 30 Jan. 1996, Appl. 94/191, 099, 21 Jul 1994; 5 pp(Japan).

[20] 20. Xu,Y., Wang,S. and Qiu,Z. (Peop. Rep. China); Faming Zhaunli Shenqing Gongkai Shuomingshu CN. 1,111,213 (C1 C01B 31/36), 8 Nov 1995, Appl. 94,114,319, 30 Dec. 1994; 7 pp (Ch.)

[21] Vlasov,A.S., Zakharov,A.I., Sakisyan,O.A. and Lukasheva,N.A.; Ogneupory 1991, (10), 15-17 (Russ.).

[22] Patel,M.; Silic. Ind. 1991, 55(1-2), 33-40(Eng.).

[23] Martinelli,J.R. and Bressiani,A.H.A.; Ceramica Isao Paulo 1989, 35(238), 162-4 (Port.).

[24] Zhang,Y., Xiao,Z. and Miao,S. (Jingdezhen Ceramics College) Faming Zhuanli Shenqing Gongkai Shuomingshu CN 1,064,069 (C1 C04B 38/06), 02 Sep. 1992, Appl. 91,100,809, 05 Feb. 1991; 7 pp.

[25] Guiterrez,R.M.De. and Delvasto,S.; Adv. Sci. Technol. 1995, 3A (Ceramics : Charting the Future), 255-62 (Eng.).

[26] Yu,Jinwei, Xu,Guanhuai, Zhao,Guopeng and Shan,Siran,; Guisuanyan Tonghao, 1996, 15(3), 48-51 (Ch.).

[27] 27. Wei,X., Lu Changhe, Fan,G. and Shi,J. (Hefei Union University); Faming Zhuanli Shenqing Gongkai Shuomingshu CN 86,107,192 (CI. CO4B 14/04), 11 may 1988, Appl. 12 oct. 1986, 5 pp.

[28] Liu Zhongcai; Faming Zhuanli Shenqing Gongkai Shuomingshu CN !,090,306 (C1. C09C 1/28), 03 Aug. 1994, Appl. 93,103,043, 20 Mar. 1993, 11 pp.

[29] Usmani,T.H., Ahmad,T.W. and Yousufzai,A.H.K.; Bioresour. Technol., 1994, 48(1), 31-5 (Eng.)

[30] Ahmedna,M., Johns,M.M., Clarke,S.J., Marshall,W.E. and Rao,R.M.; J. Sci. Food Agric. 1997, 75(1), 117-124.

[31] Youseef,A.M., Mustafa,M.R. and Dorgham,E.M.; Afinidad, 1990, 47(425), 41-4.

[32] Iwatama,Seiki (Iwayama Seiki, Japan), Jpn. Kokai Tokkyo Koho Jp. 08 62,106 [96 62,106] (C1. G01N 1/28), 8 Mar. 1996, Appl. 94/225,606, 25 Aug. 1994; 7 pp.(Japan).

[33] Shiraishi,T., Kimuraaa,M. and Ozasa,H. (Tokuyama Soda Kk), Jpn. Kokai Tokkyo Koho Jp. 05 01,184 [93 01,184] (C1. C08L 23/10), 08 Jan. 1993, Appl. 91/156,520, 27 Jun. 1991; 4 pp.

[34] Ueda,Y. and Tachino,S. (Yuu Esu Kk), Jpn. Kokai Tokkyo Koho Jp. 05 92,057 [93 92.057] (C1. A63B 57/00), 16 apr. 1993, Appl. 91/280,342, 02 Oct. 1991; 4 pp.

[35] Watanabe,J. and Sugimoto,H.Y. (Shinagawa Refractories Co. Ltd.), Jpn. Kokai Tokkyo Koho Jp. 01,224.273 [89 224,273] (C1. C04B 35/66), 07 Sep. 1989, Appl. 88/45,951, 01 Mar. 1988; 4 pp.

[36] Bhattacharya,K.K. and Chatarjee,A.K.(Council for Scientific and Industrial Research) Indian IN 164,775 (C1. C08J3/00), 27 May 1989, Appl. 85/De1125, 31 Dec. 1985; 12 pp.

[37] Painuli,D.K. and Abrol,I.K.; Catena, 1988, 15(3-4), 229-39 (Eng.).

[38] Hara,N., Inoue,N., Yamada,H., Takahashi,T. and Shibahara,K. (Agency of Ind. Sciences and Technology, Osaka Packing Mfg. Co. Ltd.); Jpn. Kokai Tokkyo Koho Jp. 63 89,499 [88 89,449] (C1 C04B 28/18), 20 Apr. 1988, Appl. 87/227,676, 10 Sep. 1987; 9 pp.

[39] Ookawachi,K. (Suruga Kogyo Kk, Japan); Jpn. Kokai Tokkyo Koho,Jp. 08,231,98 [96,231,986] (CI. C11D 3/382), 10 Sep. 1996, Appl. 95/38, 908, 28 Feb. 1995, 4 pp(Jpn.).

[40] Khatilovich,A.A., Volchanova,M.N., Farenyuk,R.M., Pribytkova,V.M. and Grunina,N.V. Derevoobrab. Prom-St., 1991. (8), 9-10 (Russ.).

[41] Yokota,J., Ishibashi,K., Yamada,K. and Tanaka,S. (Kogyo Gijuttsuin, Japan) Jpn. Kokai Tokkyo Koho Jp 08 26,875 [96 26,875] (C1. C05G 3/00), 30 Jan. 1996, Appl. 94/181,752, 11 Jul. 1994; 5 pp (Japan).

[42] Nandadasa,P.N.; Brit UK Pat. Appl. GB2,272,903 (C1. C08L 99/00), 01 Jun. 1994, LK Appl. 10,450, 20 Nov. 1992; 22 pp.

[43] Yamada,K., Ogata,T., Noda,Y., Nakagawa,K., Haraguchi,K., Ishibashi,K., Caballero,A.R., Vsita,M.T. and Manalo,L.A.; Hokkaido kogyo Kaihatsu Shikensho Hokoku 1988, (46), 23-56 (Eng.)

[44] Cowx. Peter (Elkem A/S,Norway),U.S US 5,634,960 (C1. 75-10.42;C21B11/10),3 Jun. 1997, Appl. 389,359, 16 Feb. 1995; 5 pp. (Eng.)

[45] Suzuki,K. (Nippon Tekunikusu Kk, Japan) Jpn. Kokai Tokkyo Koho Jp 08 03,610 [96 03.610] (C1. C21C 1/00), 9 Jan. 1996, Appl. 94/156,781, 15 Jun. 1994; 4 pp. (Japan).

[46] Das Gupta,Prahlad; Indian IN 168,183 (C1. C21B 13/00), 16 Feb. 1991, pl. 88/B0229 16 Aug. 1988.

[47] Barkakati,P., Bordoloi,D. and Borthakur,P.Ch.; Cem. Concr. Res. 1994, 24(4), 613-20 (Eng.)

[48] Sugita,S., Yu,Q., Shoya,M., Tsukinaga,Y. and Isojima,Y.; Proc. Int. Congr. Chem. Cem., 10th 1997, 3, 3ii109,9 pp. (Eng.).

[49] Barkakati,P., Bordoli,D., Borthakur,P.Ch. and Borah,U.C.; Trans. Indian Ceramic Soci., 1989, 48(2), 36-8 (Eng.).

[50] Singh,N.B., Bhattacharjee,K.N. and Shukla.A.K.; ZKG Int. 1997, 50(10), 594-596, 598, 600 (Eng.).

[51] Amer,A.A., El-Didamony,H., El-Hemaly,S.A.S. and El-Alfis; Silic. Ind. 1997, 62(7-8), 141-147 (Eng.), Silicates Industriels.

[52] Bhattacharya,K.K. and Chaterjee,A.K. (Council for Scietific and Industrial Research) Indian IN 164,775 (C1. C08J 3/00), 27 May 1989, Appl. 85/De1125, 31 Dec. 1985; 12 pp.

[53] Klatt,C. and Ziech,F.; Ger. DE 19,607,963, 1 Mar. 1996; 3 pp. (Ger.).

[54] Kaplunova,T.S. and Abduazimov,Kh.A.; Khim. Prir. Soedin. 1995, (4), 611-613 (Russ.).

[55] Moya,P.M.E., Duran,C.M. and Sibaja,B.R.; Ing. Cienc. Quim., 1988, 12(1-2), 24-7 (Span).

[56] Wang.S., Yuan,S., Yang.J., Zhang,J. and Shi.E.; Weishengwuxue Tongbao 1995, 22(6), 354-57 (Ch.).

[57] Haq,Q.N., Hannan,A. and Hoque,M.M.; J. Sci. Ind. Res. 1988, 23(1-4), 163-8(Eng.).

[58] Filatova,A.M., Nikolaeva,N.S., San'kova,N.B., Eremenko,Yu.S., Khomenko,N.D. and Evlanova,A.G.; Gidroliz Lesokhim. Prom-St. 1991, (7), 17-18 (Russ.).

[59] Statalov,A.A. and Kholkin,Yury I.; Int. Symp. Wood. Pulping Chem., 8th 1995, 2, 483-488.

[60] Said,O.B., Shalmor,M.B. and Egila,J.N.; Bioresour Technol. 1993, 43(1), 63-5(Eng.).

[61] Sobolev,V.I., Morozov,E.F. and Kebich,M.S.; Izu. Vyssh. Uchewn. Zaved., Cesn. Zh. 1988, (3), 73-6(Russ.)

[62] Mane,J.D., Jadhav,S.J. and Ramaiah,N.A Indian IN 160,865 (C1 C07C 55/06), 08 Aug. 1987, Appl. 85/B0248, 13 Sep. 1985, 14 pp.

[63] Williams,P.T. and Besler,S.; J. Anal. Appl. Pyrolysis, 1994, 30(1), 17-33 (Eng.).

[64] Nikunov,G.K., Burkovskaya,L.F., Artamonova,N.A. and Chelokhsaeva,G.L ; Gidroliz, Lesokhim Prom-St., 1990, (7), 18-19 (Russ.).

[65] Suda,M. (Suda Takeko, Japan); Jpn. Kokai Tokkyo Koho Jp. 08,104,513 [96 104,513] (C1. C01B 33/18), 23 Apr. 1996, Appl. 94/276, 940, 4 Oct. 1994; 2 pp.(Japan).

[66] Mao,D. and Wang,G.; Hunan Shifan Daxue Ziran Kexue Xuebao 1990, 13(2), 137-40 (Ch.).

[67] Patel,M. and Prasanna,P.; Interceram. 1991, 40(5), 301-3 (Eng.).

[68] Shimokawa,K., Sekiguchi,H., Suzuki,Y. and Ueda,Y. (Kogyo Gijutsuin); Jpn. Kokai Tokkyo Koho Jp. 05 43,208 [93 43,208] (C1. C01B 21/068), 23 Feb. 1993, Appl. 91/229,634, 16 Aug. 1991, 4 pp.

[69] Chen.J.M. and Feg.W.; Part A, Phys. Sci. Ehg. 1991, 15(5), 412-50 (Eng.).

[70] Ikram.N. and Akhter.M.; J. Mater. Sci. 1988, 23(7), 2379-81 (Eng.).

[71] Nakagawa,M.; Kogyo Zairo 1997, 45(7), 82-88.

[72] Nandi,K.C., Mukherjee,D., Biswas,A.K. and Acharya,H.N.; J. Mater. Sci. Lett. 1993, 12(16), 1248-50 (Eng.).

[73] Bayer,R., Boettger,G., Hiller,R., Huber,M., Koernig,W. and Fritz,W. (BASF A,-G.); Ger. Offen. DE 3,623,922 (C1. A23K 1/16), 21 Jan. 1988, Appl. 16 Jul. 1986, 4 pp.

[74] Lin,K.S., Wang,H.P., Huang,L.K., Hwang,C.Y. and Huang,Y.J.; Proc. Int. Conf. Solid Waste Technol. Manage. 1997, 13th (Vol. 1), paper 3C/4, 1-7.

[75] Popoola,Adeola V.; Pak. J. Sci. Ind. Res., 1996, 39(9-12), 206-208.

[76] Hevia,Roberto and Hevia,Juan Pablo; Ceram. Crist., 1997, 37(121), 28-31.

[77] Salvi,G; Riv. Combus., 1991, 45(7-8), 242-6 (Ital.).

[78] Chowdhary,R., Chakravorty,M. and Bhattacharya,P.; Int. J. Energy Res., 1991, 15(7), 593-602 (Eng.).

[79] Nijaguna,B.T, and Chapgaon,A.N.; Reg. J. Energy, Heat mass transfer, 1989, 11(2), 109-12 (Eng.).

[80] Manurung,R.K. and Beenackers,A.A.C.M.; Adv. Thermochem. Biomass Convers. [Ed. Rev. Pap. Inst. Conf.], 3rd 1993 (Pub.1994), 288-309 (Eng.).

[81] Charles N. Satterfield, Heterogeneous Catalysis in Practice, McGraw-Hill Book Company, USA, 1980.

[82] D.K.Chakraborty, Adsorption and Catalysis, Central Library, IIT Bombay, 1981.

[83] J.M.Thomas and R.M.Lambert, Characterisation of Catalysts, John Willey and Sons, Great Britain, 1980.

[84] John W. Hasler, Purification with Activated Carbon, Chemical Publising Co., New York, 1974.